

Supplementary Material for “**New Middle Miocene Ape
(Primates: Hylobatidae) from Ramnagar, India Fills
Major Gaps in the Hominoid Fossil Record**”

**Christopher C. Gilbert^{1,2,3,4*}, Alejandra Ortiz^{5,7}, Kelsey D. Pugh^{3,6},
Christopher J. Campisano^{7,8}, Biren A. Patel^{9,10}, Ningthoujam Premjit
Singh¹¹, John G. Fleagle¹², and Rajeev Patnaik¹¹**

¹Department of Anthropology, Hunter College of the City University of New York, 695 Park Avenue, New York, NY 10065

²PhD Program in Anthropology, Graduate Center of the City University of New York, 365 Fifth Avenue, NY 10016, USA

³New York Consortium in Evolutionary Primatology, New York, NY, USA

⁴Division of Paleontology, American Museum of Natural History, Central Park West at 79th Street, New York, NY, 10024, USA

⁵Department of Anthropology, New York University, New York, NY 10003

⁶Division of Anthropology, American Museum of Natural History, Central Park West at 79th Street, New York, NY, 10024, USA

⁷Institute of Human Origins, Arizona State University, Tempe, AZ 85287

⁸School of Human Evolution and Social Change, Arizona State University, Tempe, AZ 85287

⁹Department of Integrative Anatomical Sciences, Keck School of Medicine, University of Southern California, Los Angeles, CA 90033

¹⁰Human and Evolutionary Biology Section, Department of Biological Sciences, University of Southern California, Los Angeles, CA 90089

¹¹Department of Geology, Panjab University, Chandigarh, 160 014

¹²Department of Anatomical Sciences, Stony Brook University, Stony Brook, NY 11794

*Corresponding author, E-mail address: cgilbert@hunter.cuny.edu

Table of Contents

1. Detailed Materials and Methods	3
<i>Geological background</i>	3
<i>Samples</i>	5
<i>Image data acquisition</i>	7
<i>Geometric morphometric analysis</i>	8
<i>Phylogenetic analysis</i>	10
2. Extended Description of VPL/RSP2 and Diagnosis of <i>Kapi ramnagarensis</i>	12
3. Extended Results and Discussion	21
<i>2D GM analyses</i>	21
4. Additional references cited in the Supplementary Materials	24
5. Supplementary Figures and Tables	27
Figure S1	27
Table S1	28
Table S2	29
Figure S2	33
Figure S3	34
Table S3	35
Table S4	39
Table S5	43
Figure S4	45
Figure S5	46
Table S6	47
6. Supplementary Data	
Dataset S1: Chars. used in this study with char. state definitions	Separate file
Dataset S2: Matrix used for parsimony phylogenetic analysis	Separate file
Dataset S3: MorphoJ Input file for M ₃ data set	Separate file
Dataset S4: MorphoJ Input file for M ₁ data set	Separate file

1. Detailed Materials and Methods

Geological background

Outcrops of the Lower Siwalik Subgroup occur around the town of Ramnagar (figure 1), and are exposed in the southern limb of the Udhampur Syncline [51]. The southern limb of the Udhampur Syncline exhibits a continuous succession of the Siwalik Group trending N-NNE-S-SSW strike ridges [52] that are ~ 3146 m in thickness [53]. The Lower Siwalik Mansar Formation is subdivided into the lower Dodenal and the upper Ramnagar members, which have been equated to the Kamliyal and Chinji formations of the Potwar Plateau, Pakistan, respectively [53-54]. However, fauna characteristic of the Kamliyal Formation has yet to be recovered from Ramnagar [55], and the Ramnagar fauna has always been noted as similar to the Chinji Formation instead [52, 55-61]. Thus, the sedimentary deposits surrounding Ramnagar have been assigned to the Ramnagar Member of the Mansar Formation, Siwalik Group [53-54].

As previously documented [14-15, 52], the stratigraphic sequence of the study region is characterized by a repetitive sequence of major sandstones (~2-6 m thick) alternating with thick packages of reddish-brown mudstones/paleosols (~5-25 m thick) and thinner sandstones (<1 m thick) representing a successive series of fluvial channels (sandstones) and overbank/floodplain deposits (mudstones/paleosols). *Kapi* specimen VPL/RSP2 was surface collected from paleosol outcrops at the site of Sunetar 2 (figure 1). This discovery location is only ~110 m southeast from where the sivaladapid *Ramadapis sahnii* specimen VPL/RSP1 was also collected [14]. Stratigraphically, VPL/RSP2 was discovered ~10 m above VPL/RSP1, but both specimens are presumed to have been derived from the exposed 20 m thick sequence of paleosols that is bracketed by major

sandstones. Sunetar 2 correlates well with Sunetar 1 that is richly fossiliferous and is exposed ~1.2 km northwest of the former [14]; additionally, Sunetar 2 is located ~4.65 km west of Rashole 3, the site where the *Sivapithecus indicus* specimen WIF/A 1825 was collected [15]. Based on preliminary mapping of the major sandstones in the Ramnagar region, the sandstone-bounded sequence at Rashole is either equivalent, or close to equivalent, to the sequence exposed at Sunetar 1 and 2, suggesting that *Sivapithecus*, *Kapi*, and *Ramadapis* likely co-occur at the same stratigraphic level. In either case, the same biochronological constraints assigned to Rashole can be applied to Sunetar 2; stratigraphically, both sites lie slightly below the rodent-bearing site of Dehari, which has been estimated to be ~13.6-13.2 Ma on the basis of currently identified, although fragmentary, time-sensitive micromammals [17, 62]. The collected Rashole and Sunetar macromammals *Dorcabune* cf. *anthracotherioides*, *Conohyus* cf. *sindiensis*, and *Sivapithecus indicus* also have well-established first appearance dates (FADs) on the Potwar Plateau (~13.6, 14.6, and 12.7 Ma, respectively) [11, 63]. In combination with the younger end of the chronological range of the micromammals currently identified from Dehari (~13.2 Ma), we suggest that an approximate age close to 13 Ma and an estimated range of anywhere between ~12.5-13.8 Ma is most reasonable for Sunetar and Rashole (see also [15]). This is also consistent with the tip-dating analysis estimate of 11.2-14.1 Ma (95% confidence intervals, mean = 12.8 Ma) independently derived from the phylogenetic position of *Ramadapis sahnii* from Sunetar 2 (14).

Samples

The taxonomic status and phyletic affinities of VPL/RSP2 (Vertebrate Paleontology Laboratory/Ramnagar Sunetar Primate-2) and H-GSP 8114/609 were assessed using a large comparative dataset of extinct and extant catarrhine taxa. Our higher-level taxonomy (i.e., family level and above) of fossil catarrhines follows ref. [6] and is provided in tables S2 and S4. Descriptions of VPL/RSP2 were facilitated by 3D surface scans rendered from μ CT scans (Fig. 3; voxel resolution = 0.011 mm).

VPL/RSP2 corresponds to a right third lower molar (M_3) found at Sunetar 2, a site within the larger site complex of Sunetar located ~4.5 km S/SE of the town of Ramnagar, Jammu and Kashmir, India. Specimen H-GSP 8114/609 is a first lower molar (M_1) germ from the Manchar Formation in southern Pakistan and with an estimated age close to the Early/Middle Miocene boundary, ~16-17 Ma [38]. This specimen (along with a handful of other isolated teeth from the Manchar and Kamlial Formations) was referred to *Dionysopithecus* sp., a genus now recognized within the family Pliopithecidae (superfamily Pliopithecoidea), but with noted resemblances to East African Early Miocene taxa (dendropithecids and proconsulids) such as *Micropithecus*, *Proconsul*, and *Afropithecus* as well [38]. While VPL/RSP2 represented the main focus of this study, the affinities of H-GSP 8114/609 were reexamined given its proximity in time and space to the M_3 from Ramnagar and given that it is the most taxonomically informative specimen assigned to the Manchar and Kamlial Formation *Dionysopithecus* sp. hypodigm [37-39].

The comparative dataset comprises 332 molar teeth, including 71 fossil specimens from broad taxonomic categories (genera included in each category in parentheses): Propliopithecidae (*Aegyptopithecus* and *Propliopithecus*), Proconsulidae (*Ekembo*,

Equatorius, *Kalepithicus*, *Otavipithecus*, *Proconsul*, and *Rangwapithecus*), Dendropithecidae (*Dendropithecus*, *Limnopithecus*, *Micropithecus*, and *Simiolus*), Pliopithecidae (*Anapithecus*, *Dionysopithecus*, *Egarapithecus*, *Epipliopithecus*, *Laccopithecus*, *Platodontopithecus*, *Plesiopithecus*, and *Pliopithecus*), and Hylobatidae (*Yuanmoupithecus* and *Bunopithecus*). Sample size details per taxonomic category and molar type are provided in tables S2 and S4. Fossil data were collected either on the original specimens or high-resolution casts located at the following institutions: American Museum of Natural History (AMNH), New York, USA; Museum of Comparative Zoology (MCZ), Cambridge, USA; New York University (NYU), New York, USA; Arizona State University (ASU), Tempe, USA.

Our extant sample included 151 hylobatid molars from all four living genera (*Hylobates*, *Hoolock*, *Nomascus*, and *Symphalangus*) and 110 hominid molars from all three living genera (*Pongo*, *Gorilla*, and *Pan*) (tables S2 and S4). All specimens in this sample were collected from skeletal collections at the following institutions: AMNH; MCZ; National Museum of Natural History (NMNH), Washington D.C., USA; Institute of Zoology (IOZ), Chinese Academy of Sciences, Beijing, China; Kunming Institute of Zoology (KIZ), Chinese Academy of Sciences, Kunming, China; Sun Yat-sen University (SYS), Guangzhou, China, and Museum für Naturkunde (ZMB), Berlin, Germany. Sex was not included as a variable in this study. No antimeres were included and if both the right and left sides of a given specimen and molar type were available, only the best preserved was analyzed.

Image data acquisition

All analyses were conducted on high-resolution images of the occlusal surface of teeth taken with either a Canon Digital Rebel XT camera with a 75–300 mm lens, Nikon D1H camera with an A/F micro-Nikkor 105 mm lens, or a Leica EZ 4D microscope built-in camera. Following protocols described elsewhere [64-65], each tooth was oriented independently, so that the buccal, and where possible, distal portion of the cervical line was perpendicular to the optical axis of the camera. A millimeter scale placed at the same horizontal plane as the cusp apices was included in each image for calibration when using the digital cameras, and both the camera and scale were leveled using standard bubble devices. The Leica EZ 4D was equipped with a built-in calibration tool such that no external scale was necessary. To test for error in orientation between observers and devices used, we calculated the maximum crown area of six hylobatid molars with different degrees of dental wear and preservation (including one molar with missing enamel on its mesial portion due to postmortem damage and whose enamel had therefore to be digitally reconstructed) photographed independently by AO (Canon Digital Rebel XT camera) and CG (Leica EZ 4D). Sessions between observers were separated by at least one year and the percentage difference was on average 2.79%.

All digital images of the molars were imported into Adobe® Photoshop CC 2017 to align the central groove with the y-axis and the main buccolingual groove with the x-axis. Right teeth were mirror-imaged to correspond to the left side and treated as such for landmark digitizing and analyses. When necessary, interproximal wear was corrected following ref. [66]. For standardization across specimens, linear measurements and

breadth-length indices were collected from surface renderings or digital photos of VPL/RSP2 and H-GSP 8114/609 and used in comparisons across taxa. Measurements of these specimens were also taken in three dimensions (3D) using digital calipers, accounting for differences in the given descriptive measurements (3D) and those used for breadth-length indices (2D).

Geometric morphometric analysis

We used geometric morphometric techniques to quantify and visualize 2D dental shape variation in VPL/RSP2, H-GSP 8114/609 and our comparative sample. To do so, a methodological approach using homologous landmarks derived from ref. 18 was undertaken. As detailed in table S1 and figure S1, this approach included a total of 14 landmarks placed at the tips of the five main cusps (protoconid, metaconid, hypoconid, entoconid, and hypoconulid), at the intersection of main grooves, and at the intersection of the main grooves (or their projection) with the molar outline. Landmark digitizing was conducted by AO using TpsDig 232 software [67]. Intra-observer error in landmark digitizing is negligible, with further details described elsewhere [4, 68].

To minimize any taxonomic attributions based exclusively on size, we focused on shape variables in all morphometric analyses. Landmark data were imported into MorphoJ and superimposed using a generalized least-square Procrustes superimposition to remove the effects of translation, rotation, and scaling of the raw coordinate data. To test for any significant allometric component in the morphometric data, a multivariate regression of the Procrustes coordinates (dependent variables) vs. log centroid size (independent variable) was performed in MorphoJ and the relationship was found to be

non-significant with size explaining only 1.22% of the shape variance in the M_3 analysis ($p= 0.0602$). Although allometric variation is stronger and statistically significant for M_1 , only 6.99% of the shape variance can be explained by allometric effects ($p<0.001$).

Analyses were then performed on M_3 and M_1 separately. For each molar type, we first conducted a Principal Component Analysis (PCA) using the Procrustes coordinates to explore data point distribution in the shape space. Wireframe models were created within the software packages MorphoJ [20] and Morphologika2 [21] to visualize the extreme landmark configurations and determine the aspects of shape most correlated with the first and second principal components.

We also used Discriminant Function Analysis (DFA) pairwise tests, as implemented in MorphoJ, to investigate and visualize M_3 shape differences between VPL/RSP2 and each of the six major catarrhine groups included in our comparative sample (i.e., propliopithecids, proconsulids, dendropithecids, pliopithecids, hylobatids, and hominids). Procrustes distances were used to quantify the magnitude of these differences, with significance set at $p < 0.05$. It should be noted that this test differs from the classic DFA in that it allows comparisons between sample mean differences between pairs. We employed deformation grids to visualize shape deformations from the mean shape configuration (reference configuration) of each of our family-level taxonomic groups (i.e., propliopithecids, proconsulids, dendropithecids, pliopithecids, hylobatids, and hominids) to the tooth shape of VPL/RSP2 (target configuration), as well as wireframes to compare VPL/RSP2 shape with that of group means (see figure S3). DFA pairwise tests were employed in the same manner for the M_1 sample to compare H-GSP 8114/609 to the mean shape of each family-level group as well (figure S5).

Finally, hierarchical phenetic trees were obtained from Procrustes distances by means of a neighbor-joining (NJ) cluster analysis with propliopithecids used as the outgroup at the root of the tree. Support values on the branches were quantified via a 10,000 replication bootstrap procedure. All analyses were performed in MorphoJ [20], SPSS v.25 (IBM Corp., Armonk, NY) and PAST v. 3.20 [69].

Phylogenetic analysis

In addition to general qualitative and 2D morphometric analyses, we conducted a parsimony analysis of 272 morphological characters to assess the phylogenetic position of *Kapi* and *Yuamnoupithecus* within the broader catarrhine radiation (see dataset S1). While both *Kapi* and *Yuamnoupithecus* are fragmentary and only represented by aspects of their dentition, sampling a broad number of characters and fossil taxa increases the probability of sampling critical cranial and postcranial morphologies that help drive polarity assessments of important features [70-72, 90-91]. In fact, multiple studies have demonstrated that increasing the number of characters in an analysis generally increases phylogenetic accuracy and that missing data is not a serious problem as long as character sampling is sufficiently robust [73-78]. Recent studies have affirmed that even fragmentary taxa can be phylogenetically informative and that fossil taxa, in particular, can be highly beneficial and influential in analyses due to their unique combinations of character states that affect resulting topologies [78, 90-91]. While caution is always necessary when analyzing very fragmentary taxa, and while it is true that they can act as wildcards in phylogenetic analyses and significantly reduce resolution [78], in our view

the benefits of including fossil taxa, even those that are fragmentary, most often outweigh the potential negatives.

Thus, the morphological character matrix of ref. 19 was supplemented with eight new characters: seven characters derived from the results of our morphometric analyses presented above as well as recent discussions of hylobatid origins [7], and one body size character (as suggested by lower molar size, see dataset S1). In some cases, character states and scores differed from the datasets from which they were derived based on our independent qualitative and quantitative assessments of morphology (see dataset S1). *Kapi* and *Yuanmoupithecus* were scored and added to the matrix based on our own data and observations as well as information kindly provided by Terry Harrison and from the literature. All characters and character states are provided in dataset S1 and the matrix is provided as a Nexus file in dataset S2. In total, 272 characters scored for 49 taxa were included in the analysis, incorporating characters of the skull, dentition, and postcranium. *Kapi* and *Yuanmoupithecus* were scored for 16 and 38 available characters, respectively.

Characters were considered ordered whenever it can be assumed that a population likely passed through an intermediate state to get to an extreme state at either end of the character state transformation series. In these cases, ordering characters is a much more reasonable estimate of the evolutionary process (e.g., a population does not typically evolve from a small body mass to a large body mass without passing through an intermediate body mass through directional selection). Polymorphisms were coded as intermediate states between two fixed states whenever possible; simulations suggest that this coding system increases the accuracy of the resulting trees (79). All other characters

were left unordered, and all characters were left unscaled so that all steps in the analysis were given equal weight.

The resulting matrix was analyzed using maximum parsimony optimization in the program TNT (80) using traditional search methods (subtree pruning and regrafting [SPR] and tree bisection and reconnection [TBR]). Heuristic searches were performed across 10,000 replicates. Bootstrap values (1000 replicates) were calculated to assess node support. A sample of platyrrhines (*Aotus*, (*Cebus*, *Saimiri*)) along with the primitive catarrhines *Catopithecus* and *Aegyptopithecus* were constrained as successive outgroups, with the ingroup composed of *Saadanius*, pliopithecids, Old World monkeys, dendropithecids, proconsulids, *Pliobates*, hylobatids, fossil hominids (*Sivapithecus*, *Kenyapithecus*, *Pierolapithecus*, *Hispanopithecus*, *Ouranopithecus*, *Lufengpithecus*, and *Oreopithecus*), and extant hominids (*Pongo*, *Gorilla*, and *Pan*). Broad-level taxonomy follows the main text [6].

2. Extended Description of VPL/RSP2 and Diagnosis of *Kapi ramnagarensis*

Extended Description

VPL/RSP2 corresponds to a relatively low-crowned M₃ with rounded corners from a catarrhine primate slightly smaller than *Hoolock* in molar size. VPL/RSP2 is mesiodistally longer than broad (breadth-length index of 0.79), indicating proportions within the range of extant hylobatids and most similar to those of proconsulids among fossil catarrhine taxa (mean breadth-length index of 0.77; range 0.68-0.85). It is considerably broader, on average, than those of pliopithecids (0.74; 62-87), and slightly broader than those of modern *Symphalangus* (0.75; 0.71-0.81), propiopithecids (0.75;

0.70-0.83), and dendropithecids (0.76; 0.71-0.83); however, it is relatively narrow compared to many modern gibbons (*Nomascus* = 0.85; 0.81-0.89, *Hoolock* = 0.84; 0.78-0.89, and *Hylobates* = 0.85; 0.77-0.92), as well as those of extinct *Yuanmoupithecus* (0.81) and *Bunopithecus* (0.82).

The crown of VPL/RSP2 is ovoid in occlusal outline, tapering distally such that its distal moiety is narrower than its mesial moiety. There are five well-developed cusps, arranged around the periphery of the crown. Cusps are low and conical in shape. The buccal wall of the crown shows some bulging and a moderately expressed semi-continuous buccal cingulum. The metaconid is the most voluminous (28% of total crown) and highest cusp, followed by the hypoconid and protoconid (25% and 22% of total crown area, respectively), which are subequal in elevation. The entoconid is similar in elevation to the hypoconid and protoconid, but relatively smaller in basal area (14% of total crown area). The hypoconulid is the smallest (11% of total crown area) of the five cusps. The hypoconulid is more distally placed relative to the hypoconid and entoconid and located slightly towards the buccal side of the midline of the crown.

The protocone has short but well-developed preprotocristid and postprotocristid. The metaconid is slightly mesial to the protoconid and has a short and rounded premetacristid. The metaconid and entoconid are widely spaced by a long postmetacristid. The hypoconid has a short prehypocristid (cristid obliqua) that is parallel to the long axis of the crown (rather than slightly oblique). Both the postentocristid and the posthypoconulid cristid are low and ill-defined, possibly due to moderate wear. The mesial fovea (i.e., trigonid basin) is long and rectangular, delimited distally by a well-differentiated hypometacristid and hypoprotocristid. The mesial marginal ridge is

relatively sharp and well-developed. The distal fovea is intermediate in size but poorly defined.

The basal area of the trigonid is similar to the talonid. The talonid basin is expansive and has a simple Y-shaped groove pattern with no secondary wrinkling. A well-developed postcristid and hypoentocristid form the mesial-most portion of the distal fovea, separating it from the talonid basin. The metaconid is damaged, but there may be traces of a small mesostylid on the postmetacristid. A small tubercle is also present on the preprotocristid. There is no evidence of a pliopithecine triangle and no retention of the paraconid.

Extended Diagnosis and Comparisons with other taxa

Kapi ramnagarensis (VPL/RSP2) shares with hylobatids a number of synapomorphies: simple and low-crowned molars with rounded corners; peripherally arranged cusps; low conical cusps; absence of secondary wrinkling; weak crest development; expansive talonid basin; poorly defined distal fovea (but one that is intermediate in size vs. extant hylobatids that have a small/pit-like fovea); patterns of cusp proportions in which the protoconid, metaconid and hypoconid are roughly equal in basal area and more voluminous than the entoconid and hypoconulid; very small hypoconulid that is situated on the distal margin of the crown, slightly buccally but closer to the midline of the tooth; metaconid slightly mesial to protoconid; widely spaced metaconid and entoconid.

Compared to extant hylobatids, however, *K. ramnagarensis* exhibits: less inflated and slightly less peripherally oriented cusps, the presence of a moderately developed

buccal cingulum (buccal cingulum expression ranges from absent to poorly developed in extant hylobatids with the exception of *Nomascus*, which can exhibit moderate expressions of these features as documented by Frisch [81] and Zhang et al. [5]), a well-defined and relatively long mesial fovea, better developed occlusal crests, a more elevated mesial marginal ridge; the presence of a small mesostylid (although a small to greatly pronounced mesostylid is common in some stem catarrhines and stem hominoids [39]); and a smaller breadth/length ratio with distal tapering.

Although early accounts suggested that pliopithecids and hylobatids were closely related [82-84], subsequent studies demonstrated that pliopithecids form a monophyletic group and that resemblances between the two clades were only superficial due to similarities in size and retention of primitive features [6-7, 31-33, 39]. Pliopithecids exhibit a combination of the following key lower molar features: presence of the pliopithecine triangle (although the pliopithecine triangle can be absent or weakly expressed in the M_{1s} of pliopithecoids, it is almost always present and well-developed in their M_{3s} [39]); buccal cusps that are shifted mesially relative to the lingual cusps; buccally positioned hypoconulid, which is almost in line with the two main buccal cusps (this is the general pattern seen in extinct catarrhines, but pliopithecids show this condition to an extreme); and very long and narrower lower molars (mean breadth-length index = 0.74).

Other features generally present in primitive catarrhines (e.g., propliopithecids, proconsulids, dendropithecids, pliopithecids) not observed in VPL/RSP2 include: retention of the paraconid, elevated occlusal crests and presence of secondary wrinkling, a well-developed buccal cingulum (which sometimes includes small accessory cuspules),

a long and narrow talonid basin, a hypoconulid that is only slightly smaller than the hypoconid, higher crowned molars with tall, discrete cusps, a broad and well-defined distal fovea, and a prominent mesostylid.

More specifically, *K. ramnagarensis* differs from propioplithecid lower molars in the following features: more peripherally placed cusps, significantly reduced buccal flare, a relatively broad occlusal/talonid basin, shorter molar crown with increased bunodonty, hypoconid and entoconid more transversely aligned, metaconid typically larger than the protoconid, much larger mesial cusps compared to distal cusps (entoconid, hypoconid, and hypoconulid), a less extensive (mesiodistally) buccal cingulum that terminates more mesially (at the distal end of the hypoconid, at least on the M₃), a reduced (much smaller) and slightly more buccally positioned M₃ hypoconulid, more oval and less elongated lower M₃ crown, and the lack of a hypoconulid lobe on M₃.

Kapi ramnagarensis can be distinguished from dionysopithecine pliopithecids by: the absence of a paraconid, transversely aligned mesial and distal cusps with a transverse (rather than oblique) mesial crest between the protoconid and metaconid, a cristid obliqua that is oriented mesiodistally rather than slightly oblique, a comparatively reduced buccal cingulum with buccal cusps closer to the periphery of the tooth, a relatively broader talonid basin, a relatively shorter molar crown with increased bunodonty, the absence of a pliopithecine triangle or any crests associated with a pliopithecine triangle, metaconid typically larger than the protoconid, a relatively smaller entoconid-hypoconulid pair (and relatively larger mesial cusps compared to distal cusps), and an M₃ hypoconulid that is slightly buccal, but not connected to or in line with the other buccal cusps. The new Ramnagar ape can be distinguished from pliopithecine (*Pliopithecus* and *Epipliopithecus*)

lower molars by: more transversely aligned mesial and distal cusps with a transverse mesial crest between the protoconid and metaconid, the metaconid a more oval (less elongated and rectangular) occlusal/crown outline, a relatively smaller hypoconulid-entoconid pair, more peripherally placed cusps creating a relatively broader occlusal basin that is devoid of any crestring, a shorter molar crown and cusps with increased bunodonty, a reduced buccal cingulum that terminates more mesially, the absence of a pliopithecine triangle or any crests associated with a pliopithecine triangle, and an M₃ hypoconulid that is only slightly buccal rather than connected to or in line with the other buccal cusps. *Kapi* differs in lower molar anatomy from crouzelines (*Plesiopliopithecus*, *Egarapithecus*, *Anapithecus*, *Barberapithecus*, and *Laccopithecus*) in the following features: a relatively shorter, broader occlusal outline with a more oval shaped (rather than elongated) M₃, transversely aligned mesial cusps with a transversely oriented crest (rather than oblique) between the protoconid and metaconid creating a transversely oriented mesial fovea, a mesially directed (rather than oblique) cristid obliqua, more peripherally placed cusps creating a relatively broad occlusal basin with no obvious crests or extensive enamel wrinkling (cresting/wrinkling also reduced in *Laccopithecus*), a mesiodistally reduced buccal cingulum, a shorter molar crown with increased bunodonty, more transversely aligned hypoconid and entoconid, the absence of a pliopithecine triangle or any crests associated with a pliopithecine triangle (also absent in *Laccopithecus* and possibly *Egarapithecus*), and an M₃ hypoconulid that is less buccally positioned than observed in most crouzelines (except *Laccopithecus*). While *Laccopithecus* shares with *Kapi* the absence of the pliopithecine triangle, a somewhat reduced buccal cingulum (though still mesiodistally longer than in *Kapi*), and a less

buccal hypoconulid than seen in most other pliopithecoids, it is easily diagnosed compared to *Kapi* by its elongated molar crowns, more mesially positioned buccal cusps relative to the lingual cusps, obliquely oriented mesial transverse crest and mesial fovea, more obliquely oriented cristid obliquid, and more internally placed cusps leading to a narrower and more restricted occlusal basin.

While *Kapi* is similar to the recently emended pliopithecoid genus *Krishnapithecus* in its conical, uninflated, peripherally positioned cusps, reduced flare, and broad occlusal basin, *Kapi* differs *Krishnapithecus* in its overall smaller size, transversely aligned mesial and distal cusps, transversely aligned mesial transverse crest and mesial fovea, relatively low, bunodont crown and cusp height, lack of a pliopithecine triangle and any crests associated with the pliopithecine triangle, and presence of a moderately developed buccal cingulum.

Compared to pliopithecids, *Kapi* is less easily distinguished in lower molar morphology from dendropithecoid and proconsulid taxa, which are less dentally specialized and more diverse. Still, there are clear, compelling, and diagnosable differences between *Kapi* and all well-established genera for which lower dentitions exist. *Kapi* differs from *Dendropithecus* in the following features: a relatively shorter and broader occlusal crown (on average) and more oval and less elongated/rectangular M₃, more peripherally placed cusps and less buccal flare, a relatively broader occlusal basin, more transversely aligned hypoconid and entoconid, a reduced buccal cingulum terminating more mesially (just distal to the hypoconid), less developed occlusal crests with shorter, more bunodont cusps, and an M₃ hypoconulid that is smaller and not as buccally positioned. *Kapi* contrasts with *Simiolus* in the following features: a relatively

shorter and broader occlusal crown (on average), a relatively broad occlusal basin lacking any cresting or wrinkling, reduced occlusal flare and more peripherally placed cusps, more transversely aligned mesial and distal cusps, a reduced buccal cingulum terminating more mesially (just distal to the hypoconid), less developed occlusal shearing crests with shorter, more bunodont cusps, and an M₃ hypoconulid that is smaller and not as buccally positioned. *Kapi* is differentiated from *Micropithecus* by: more peripherally placed cusps and reduced occlusal flare, a more transverse mesial fovea (rather than oblique), a relatively broad occlusal basin lacking any cresting or wrinkling, a slightly reduced buccal cingulum terminating more mesially than in most *Micropithecus* specimens, but with overlap, and an M₃ hypoconulid that is smaller and not as buccally positioned. *Kapi* is distinguished from *Limnopithecus* by: more peripherally placed cusps and reduced occlusal flare, a relatively broader occlusal basin lacking any cresting or wrinkling, a reduced buccal cingulum terminating more mesially, a broader and relatively shorter M₃ crown (on average), and an M₃ hypoconulid that is typically not as buccally positioned.

Among proconsulids, *Kapi* is much smaller than all known genera except *Kalepithicus*. *Kapi* is most clearly differentiated in lower molar anatomy from *Kalepithicus* by its more conical cusps, more transversely aligned mesial and distal cusps, reduced buccal cingulum, much reduced occlusal flare, more peripherally placed cusps leading to a broader and more open talonid basin, and a reduced M₃ hypoconulid. *Kapi* is differentiated from *Kogolepithicus* by more transversely aligned hypoconid and entoconid, a reduced buccal cingulum, more peripherally placed cusps leading to a broader occlusal basin lacking clear cresting or wrinkling, and reduced occlusal flare. In addition to its smaller size, *Kapi* is generally differentiated from other proconsuline

(*Proconsul* and *Ekembo*) proconsulid lower molars by its shorter and broader M₃, reduced buccal cingulum, more peripherally placed occlusal cusps leading to a relatively broader occlusal basin, reduced occlusal flare, and a lack of noticeable wrinkling or cresting in and around the talonid basin. *Kapi* is distinct from nyanzapithecine proconsulids in its less inflated cusps, more transversely aligned mesial and distal cusps, reduced buccal cingulum terminating more mesially, a much broader occlusal basin lacking any substantial cresting and/or enamel wrinkling, shorter and broader occlusal outline and much less elongate M₃, more centrally placed M₃ hypoconulid. *Kapi* differs from known lower dentitions of afropithecine proconsulids (*Afropithecus*, *Morotopithecus*, *Heliopithecus*, *Nacholapithecus*, *Equatorius*, and *Otavipithecus*) in the following features: much smaller size, shorter and broader occlusal outline (at least in M₃), less inflated/more conical cusps and reduced occlusal flare, relatively broader and more open occlusal basin lacking crests or enamel wrinkling, more transversely aligned hypoconid and entoconid, and the presence of a moderately developed buccal cingulum (reduced to absent in most afropithecines, although *Kapi* is similar in development to that seen in *Otavipithecus*).

Kapi is most clearly differentiated from all known hominid genera by its much smaller size. In addition, its cusps tend to be less inflated and less bundont, the mesial fovea is relatively broad and long, the crown generally exhibits reduced flare, the broad occlusal basin lacks any cresting or wrinkling, a moderate buccal cingulum is present, and the hypoconid and entoconid are typically more transversely aligned, although overlapping the known range of variation among hominids. For a visual comparison of VPL/RSP2 with a sample of other taxa, see figure S2.

3. Extended Results and Discussion

2D GM analyses

Tables S3, S5, and S6 summarize the results of the PCAs, including the eigenvalues and percentage of the variance explained by each of the 24 principal components. Figure 3 of the main text illustrates the M_3 shape variation along the first two principal components, where PC 1 accounts for 25.1% of M_3 shape variation and PC 2 explains 10.8%.

Figure 3 shows a very clear gradient along PC 1, with hylobatids occupying almost exclusively negative values, hominids spanning both positive and negative values, and stem catarrhine/hominoid groups displaying positive values for PC 1. This distribution in the morphospace leads to nearly complete overlap among propliopithecids, proconsulids, dendropithecids, and pliopithecids along PC 1, and their strong separation from hylobatids and a number of crown hominid specimens as well. In fact, negative values on PC 1 are exclusive to crown hominoid specimens, and the vast majority of those specimens are crown hylobatids. Taxa in positive morphospace along PC 1 are characterized by longer and narrower molars with closely spaced protoconid, metaconid, entoconid and hypoconid due to the more central position of the buccal cusps (i.e., protoconid and hypoconid) and an overall shift of the four main cusps slightly more mesially. This relates both to overall increased crown flare in these taxa and a strong buccal cingulum in many cases as well. Positive values on PC 1 also have a large buccally positioned hypoconulid, a more skewed configuration of the talonid, more obliquely aligned mesial and distal cusps, and a narrow area formed by the Y-shaped

groove pattern. PC 2 mainly differentiates propliopithecids from the other groups, which are widely spread in morphospace along this axis. Specimens at the positive end of PC 2 have molar crowns that exhibit less elongation and posterior tapering, while those at the negative end evince strong crown elongation and distal tapering. Other features loading on PC 2 seem to overlap with those on PC 1 and include differences in cusp position relative to the outline of the crown (i.e., flare), the position of the hypoconulid, and the relative positions of the buccal vs. lingual cusps. *Kapi* falls on negative PC 1 and negative PC 2, well within the range of variation observed among crown hylobatids and crown hominids to the exclusion of stem catarrhine/stem catarrhine groups, and plots closest to a number of hylobatid specimens. *Bunopithecus*, an extinct hylobatid from the Middle Pleistocene, plots exclusively within the hylobatid distribution, while *Yuanmoupithecus*, the earliest uncontested stem hylobatid known to date, falls within the small area of overlap among hylobatids, hominids, and dendropithecids. Interestingly, *Laccopithecus* falls exclusively within the distribution of extinct catarrhines, supporting the most common taxonomic placement of *Laccopithecus* with the Pliopithecoidea, despite early claims that it was a stem hylobatid [85-89].

The results of the PCA performed on the M_1 dataset are summarized in tables S5-S6. Figure S4 illustrates the distribution of the specimens and the relative placement of H-GSP 8114/609 along the first two principal components, where PC 1 and PC 2 account for 21.2% and 14.4% of M_1 shape variation, respectively. There is more overlap among groups in the M_1 PCA, consistent again with the suggestion that they are perhaps not as distinctive between taxa as are M_{3s} [27]. Hylobatids plot throughout negative PC 1 and the left-most portion of positive PC 1, while hominids are primarily located on positive

PC 1 with only a couple of specimens in negative PC 1 space. Stem catarrhine/hominoid taxa are spread across PC 1 and are primarily separated from crown hominoid taxa on PC 2; most propliopithecids, proconsulids, dendropithecids, and pliopithecids are found at the positive end of PC 2 and most hominids and hylobatids are found largely at the negative end. Proconsulids notably span both positive and negative PC 2 space, and dendropithecids cross into negative PC 2 space as well. Propliopithecids and pliopithecids plot exclusively in positive PC 2 space.

H-GSP 8114/609 plots on positive PC 1 and positive PC 2, in the area of overlap between dendropithecids, pliopithecids, and hominids, but to the exclusion of propliopithecids, proconsulids, and hylobatids. Specimens with negative loadings on PC 1 are characterized by narrower molar crowns with the entoconid and hypoconid more transversely aligned, increased distal tapering, a centrally positioned hypoconulid, and more peripherally placed cusps. The positive end of PC 1 appears associated with a relatively broader crown and occlusal basin, more centrally placed cusps, increased basal flare, a more mesially shifted hypoconid compared to entoconid, a more buccally positioned hypoconulid, and a lack of distal tapering. Specimens with positive PC 2 values exhibit centrally compressed cusp apices due primarily to the much more central position of the buccal cusps, more obliquely aligned buccal and lingual cusps, a much larger buccal cingulum and/or flare, and increased distal tapering. At the negative end of PC 2, M_{1S} show reduction of the buccal flare/cingulum, a broad occlusal basin, more transversely aligned buccal and lingual cusps, and less distal tapering.

Additional references cited in the Supplementary Materials

51. Gupta SS, Verma BC. 1988 Stratigraphy and vertebrate fauna of the Siwalik group, Mansar-Uttarbarani section, Jammu district, Jammu and Kashmir. *J. Palaeontol. Soc. Ind.* **33**, 117-124.
52. Basu PK. 2004 Siwalik mammals of the Jammu Sub-Himalaya, India: an appraisal of their diversity and habitats. *Quatern. Int.* **117**, 105-118. (doi:10.1016/S1040-6182(03)00120-4)
53. Gupta SS. 2000 Lithostratigraphy and structure of the Siwalik succession and its relationship with the Murree succession around Ramnagar area, Udhampur District, J & K. *Himal. Geol.* **21**, 53-61.
54. Gupta SS. 1997 Study and documentation of vertebrate fossils from the Siwalik Group of Jammu Sub-Himalayan foot hills. *Geol. Surv. Ind.* **129**, 5-7.
55. Nanda AC, Sehgal RK. 1993 Siwalik mammalian faunas from Ramnagar (J and K) and Nurpur (H.P.) and lower limit of *Hipparion*. *J. Geol. Soc. Ind.* **42**, 115-134.
56. Brown B, Gregory WK, Hellman M. 1924 On three incomplete anthropoid jaws from the Siwaliks, India. *Am. Mus. Novit.* **130**, 1-8.
57. Pilgrim GE. 1927 A *Sivapithecus* palate and other primate fossils from India. *Mem. Geol. Soc. Ind.* **14**, 1-26.
58. Colbert EH. 1935 Siwalik mammals in the American Museum of Natural History. *Trans. Am. Phil. Soc.* **26**, 1-40.
59. Gregory WK, Hellman M, Lewis GE. 1938 Fossil anthropoids of the Yale-Cambridge India expedition of 1935. *Carnegie Inst. Washington Publ.* **495**, 1-27.
60. Vasishat RN, Gaur R, Chopra SRK. 1978 Geology, fauna and palaeoenvironment of Lower Siwalik deposits around Ramnagar, India. *Nature* **275**, 736-737.
61. Gaur R, Chopra SRK. 1983 Palaeoecology of the middle Miocene Siwalik sediments of a part of Jammu and Kashmir State, India. *Palaeogeogr. Palaeocl.* **43**, 313-327.
62. Parmar V, Prasad GVR. 2006 Middle Miocene rhizomyid rodent (Mammalia) from the Lower Siwalik Subgroup of Ramnagar, Udhampur District, Jammu and Kashmir, India. *Neu. Jah. Geol. Palaeontol.* **6**, 371-384.
63. Barry JC, *et al.* 2013 The Neogene Siwaliks of the Potwar Plateau, Pakistan. In *Fossil Mammals of Asia: Neogene Biostratigraphy and Chronology* (eds. X Wang, LJ Flynn, M Fortelius), pp. 373-399. New York: Columbia University Press.
64. Bailey SE. 2002 *Neandertal dental morphology: implications for modern human origins*. Ph.D. Thesis, Arizona State Univ.
65. Pilbrow VC. 2003 *Dental variation in African apes with implications for understanding patterns of variation in species of fossil apes*. Ph.D. Thesis, New York Univ.
66. Wood BA, Engleman CA. 1988 Analysis of the dental morphology of Plio-Pleistocene hominids, V. Maxillary postcanine tooth morphology. *J Anat.* **161**, 1-35.
67. Rohlf FJ. 2016 TpsDig232. TpsSeries, Stony Brook Univ.
68. Ortiz A, Villamil CI, Kimock CM, He K, Harrison T. 2017 Tracking hylobatid taxonomic diversity from molar morphometrics. *Am. J. Phys. Anthropol.* **S64**: 306.
69. Hammer Ø, Harper DAT, Ryan PD. 2001 PAST: Paleontological Statistics Software Package for Education and Data Analysis. *Palaeontol. Electron.* **4**, 1-9. (http://palaeo-electronica.org/2001_1/past/issue1_01.htm)

70. Gatesy J, O'Leary MA. 2001 Deciphering whale origins with molecules and fossils. *Trends Ecol. Evol.* **16**, 562-570. (doi:10.1016/S0169-5347(01)02359-X)
71. Gatesy J, Amato G, Norell M, DeSalle R, Hayashi C. 2003 Combined support for wholesale taxic atavism in Gavailine Crocodylians. *Systematic Biol.* **52**, 403-422. (doi: 10.1080/10635150390197037)
72. Springer MS, Teeling EC, Madsen O, Stanhope MJ, de Jong WW. 2001 Integrated fossil and molecular data reconstruct bat echolocation. *Proc. Natl. Acad. Sci. USA* **98**, 6241-6246. (doi:10.1073/pnas.111551998)
73. Wiens JJ. 1998 Does adding characters with missing data increase or decrease phylogenetic accuracy? *Systematic Biol.* **47**, 625-640.
74. Wiens JJ. 2003 Incomplete taxa, incomplete characters, and phylogenetic accuracy: is there a missing data problem? *J. Vertebr. Paleontol.* **23**, 297-310. (doi:10.1671/0272-4634(2003)023[0297:ITICAP]2.0.CO;2)
75. Wiens JJ. 2003 Missing data, incomplete taxa, and phylogenetic accuracy. *Systematic Biol.* **52**, 528-538. (doi:10.1080/10635150390218330)
76. Wiens JJ. 2006 Missing data and the design of phylogenetic analyses. *J. Biomed. Inform.* **39**, 34-42. (doi:10.1016/j.jbi.2005.04.001)
77. Wiens JJ, Morrill MC. 2011 Missing data in phylogenetic analysis: reconciling results from simulations and empirical data. *Systematic Biol.* **60**, 719-731. (doi:10.1093/sysbio/syr025)
78. Pattinson DJ, Thompson RS, Piotrowski AK, Asher RJ. 2015 Phylogeny, paleontology, and primates: do incomplete fossils bias the tree of life? *Systematic Biol.* **64**, 169-186. (doi:10.1093/sysbio/syu077)
79. Wiens JJ. 2000 Coding morphological variation within species and higher taxa for phylogenetic analysis. In *Phylogenetic Analysis of Morphological Data* (ed. JJ Wiens), pp. 115-145. Washington, DC: Smithsonian Institution Press.
80. Goloboff PA, Farris JS, Nixon KC. 2008 TNT, a free program for phylogenetic analysis. *Cladistics* **24**, 774-786. (doi:10.1111/j.1096-0031.2008.00217.x)
81. Frisch JE. 1965 Trends in the evolution of the hominoid dentition. *Bibliotheca Primatologica Basel* **3**, 1-130.
82. Simons EL. 1972 *Primate evolution: an introduction to man's place in nature*. New York: MacMillan.
83. Simons EL, Fleagle JG. 1973 The history of extinct gibbon-like primates. *Gibbon Siamang* **2**, 121-148.
84. Wu R, Pan Y. 1985 Preliminary observation on the cranium of *Laccopithecus robustus* from Lufeng, Yunnan with reference to its phylogenetic relationship. *Acta Anthropol. Sinica* **4**, 7-12.
85. Pan Y. 1988 Small fossil primates from Lufeng, a latest Miocene site in Yunnan Province, China. *J. Hum. Evol.* **17**, 359-366.
86. Tyler DE. 1991 The problems of the Pliopithecidae as a hylobatid ancestor. *Hum. Evol.* **8**, 73-80.
87. Tyler DE. 1993 The evolutionary history of the gibbon. In *Evolving Landscapes and Evolving Biotas of East Asia since the Mid-Tertiary* (ed. NG Jablonski), pp. 228-240. Hong Kong: University of Hong Kong.

88. Nisbett RA, Ciochon RL. 1993 Primates in northern Viet Nam: a review of the ecology and conservation status of extant species, with notes on Pleistocene localities. *Int. J. Primatol.* **14**, 765–795.
89. Jablonski NG, Chaplin G. 2009 The fossil record of gibbons. In *The Gibbons* (eds. S Lappan, DJ Whittaker), pp. 111–130. New York: Springer.
90. Koch NM, Parry LA. 2020 Death is on our side: paleontological data drastically modify phylogenetic hypotheses. *Sys. Biol.* <https://doi.org/10.1101/723882>
91. Asher RJ, Smith MR, Rankin A, Emry RJ. 2019. Congruence, fossils and the evolutionary tree of rodents and lagomorphs. *R. Soc. Open Sci.* **6**, 190387. <http://dx.doi.org/10.1098/rsos.190387>

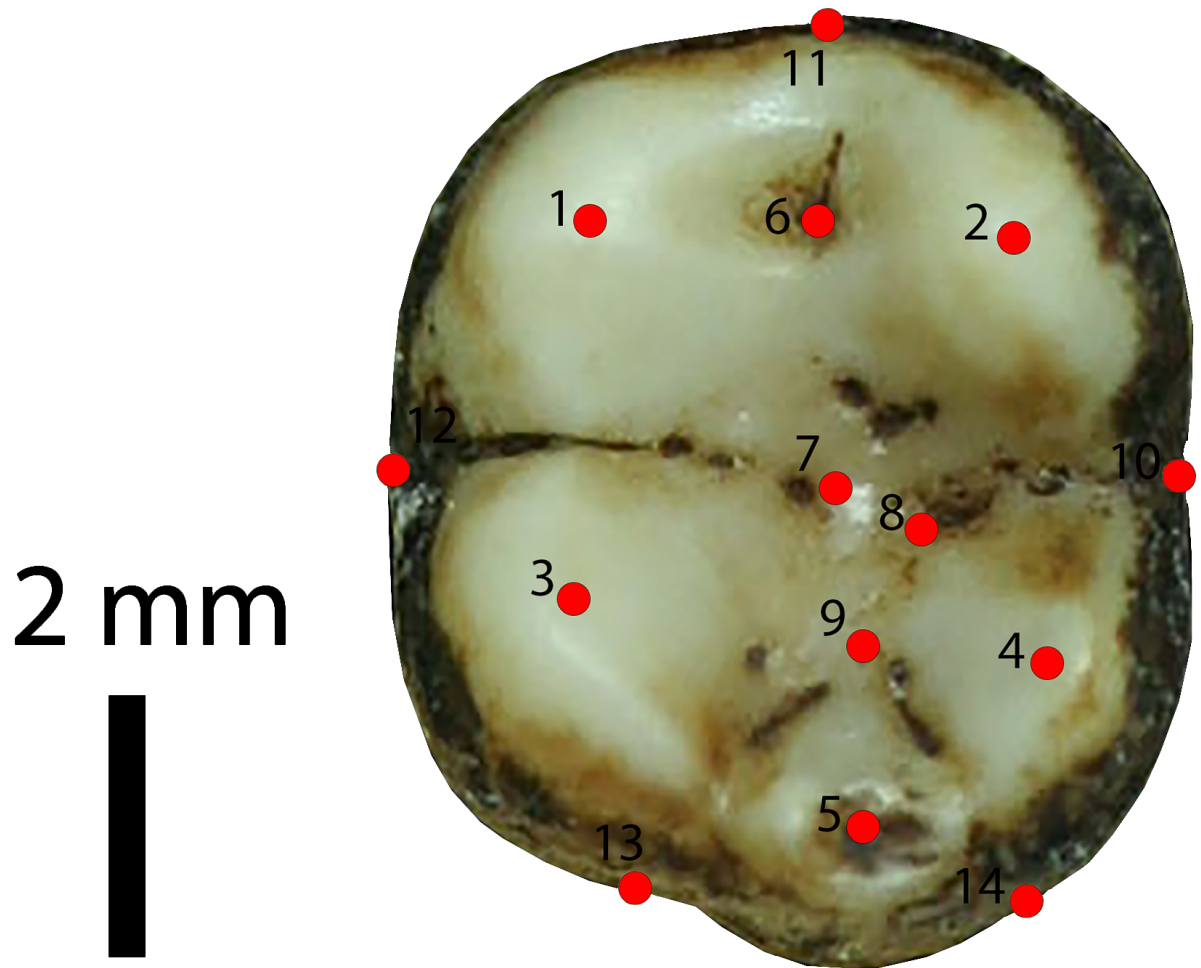


Figure S1. Protocol used in comparative analyses of catarrhine lower molars by means of 14 landmark 2D geometric morphometrics. Specimen depicted is a left M₃ of *Hoolock leuconedys*. See also Table S1.

Landmark	Description
1	Tip of the mesiobuccal cusp or protoconid
2	Tip of the mesiolingual cusp or metaconid
3	Tip of the distobuccal cusp or hypoconid
4	Tip of the distolingual cusp or entoconid
5	Tip of the hypoconulid or cusp 5
6	Center of the mesial fovea
7	Point where the central groove is crossed by the mesiobuccal groove
8	Point where the central groove is crossed by the lingual groove
9	Point where the central groove is intersected by the distobuccal groove (beginning of cusp 5)
10	Point where the dental outline is intersected by the lingual groove
11	The most mesial point of the occlusal outline opposite the mesial fovea
12	Point where the dental outline is intersected by the mesiobuccal groove
13	Point where the dental outline is intersected by the distobuccal groove
14	Point where the dental outline is intersected by the distal prolongation of the central groove

Notes: Landmark definitions based on ref 18.

Table S1. List of landmarks used in the 2D geometric morphometric analyses of occlusal morphology.

Specimen number	Family	Genus and species	Fossil/Extant
DPC 1027	Propliopithecidae	<i>Aegyptopithecus zeuxis</i>	Fossil
DPC 2806	Propliopithecidae	<i>Aegyptopithecus zeuxis</i>	Fossil
YPM 21032	Propliopithecidae	<i>Aegyptopithecus zeuxis</i>	Fossil
DPC 1028	Propliopithecidae	<i>Aegyptopithecus zeuxis</i>	Fossil
DPC 5392	Propliopithecidae	<i>Propliopithecus ankeli</i>	Fossil
DPC 1069	Propliopithecidae	<i>Propliopithecus chirobates</i>	Fossil
BM(NH).M 16650	Dendropithecidae	<i>Dendropithecus macinnesi</i>	Fossil
KNM-RU 2015	Dendropithecidae	<i>Dendropithecus macinnesi</i>	Fossil
KNM-ZP 01669b	Dendropithecidae	<i>Dendropithecus sp. indet.</i>	Fossil
KNM-SO 444	Dendropithecidae	<i>Limnopithecus evansi</i>	Fossil
KNM-ZP 01675	Dendropithecidae	<i>Limnopithecus sp. indet.</i>	Fossil
KNM-MB 9767	Dendropithecidae	<i>Micropithecus leakeyorum</i>	Fossil
KNM-WK 16960	Dendropithecidae	<i>Simiolus enjiessi</i>	Fossil
KNM-RU 7290	Proconsulidae	<i>Ekembo heseloni</i>	Fossil
KNM-RU 1674	Proconsulidae	<i>Ekembo nyanzae</i>	Fossil
KNM-RU 1947	Proconsulidae	<i>Ekembo nyanzae</i>	Fossil
KNM-SO 378	Proconsulidae	<i>Kalepithecus songhorensis</i>	Fossil
BER I	Proconsulidae	<i>Otavipithecus namibiensis</i>	Fossil
KNM-SO 396	Proconsulidae	<i>Proconsul major</i>	Fossil
KNM-SO 463	Proconsulidae	<i>Rangwapithecus gordonii</i>	Fossil
RUD 98	Pliopithecidae	<i>Anapithecus hernyaki</i>	Fossil
IPS 2943	Pliopithecidae	<i>Egarapithecus narcisoi</i>	Fossil
Naturhistorisches Museum (Basel), Individual III	Pliopithecidae	<i>Epipliopithecus vindobenensis</i>	Fossil
Naturhistorisches Museum (Basel), Individual I	Pliopithecidae	<i>Epipliopithecus vindobenensis</i>	Fossil
PA 880	Pliopithecidae	<i>Laccopithecus robustus</i>	Fossil
PA 870	Pliopithecidae	<i>Platodontopithecus jianghuaiensis</i>	Fossil
MNHN Chantrei Deperet, La Grive	Pliopithecidae	<i>Pliopithecus antiquus</i>	Fossil
Goriach (H30), Joanneum 3675	Pliopithecidae	<i>Pliopithecus platydon</i>	Fossil
MNHN Sansan (H2)	Pliopithecidae	<i>Pliopithecus sp. indet.</i>	Fossil
AMNH 18534	Hylobatidae	<i>Bunopithecus sericus</i>	Fossil
VPL/RSP-2	Hylobatidae	<i>Kapi ramnagarensis</i>	Fossil
YML 112-1x	Hylobatidae	<i>Yuanmoupithecus xiaoyuan</i>	Fossil
AMNH 112688	Hylobatidae	<i>Hoolock hoolock</i>	Extant
AMNH 112697	Hylobatidae	<i>Hoolock hoolock</i>	Extant
AMNH 112698	Hylobatidae	<i>Hoolock hoolock</i>	Extant
AMNH 112702	Hylobatidae	<i>Hoolock hoolock</i>	Extant
AMNH 112703	Hylobatidae	<i>Hoolock hoolock</i>	Extant
AMNH 83413	Hylobatidae	<i>Hoolock hoolock</i>	Extant
AMNH 83415	Hylobatidae	<i>Hoolock hoolock</i>	Extant

AMNH 83417	Hylobatidae	<i>Hoolock hoolock</i>	Extant
AMNH 112671	Hylobatidae	<i>Hoolock leuconedys</i>	Extant
AMNH 112674	Hylobatidae	<i>Hoolock leuconedys</i>	Extant
AMNH 112680	Hylobatidae	<i>Hoolock leuconedys</i>	Extant
AMNH 112683	Hylobatidae	<i>Hoolock leuconedys</i>	Extant
AMNH 112719	Hylobatidae	<i>Hoolock leuconedys</i>	Extant
AMNH 112720	Hylobatidae	<i>Hoolock leuconedys</i>	Extant
AMNH 112960	Hylobatidae	<i>Hoolock leuconedys</i>	Extant
KIZ 014035	Hylobatidae	<i>Hoolock leuconedys</i>	Extant
USNM 257988	Hylobatidae	<i>Hoolock leuconedys</i>	Extant
AMNH 102773	Hylobatidae	<i>Hylobates agilis</i>	Extant
AMNH 102774	Hylobatidae	<i>Hylobates agilis</i>	Extant
AMNH 106571	Hylobatidae	<i>Hylobates agilis</i>	Extant
AMNH 102161	Hylobatidae	<i>Hylobates agilis</i>	Extant
AMNH 102200	Hylobatidae	<i>Hylobates agilis</i>	Extant
AMNH 106572	Hylobatidae	<i>Hylobates agilis</i>	Extant
AMNH 106578	Hylobatidae	<i>Hylobates agilis</i>	Extant
AMNH 106678	Hylobatidae	<i>Hylobates agilis</i>	Extant
AMNH 106679	Hylobatidae	<i>Hylobates agilis</i>	Extant
AMNH 103442	Hylobatidae	<i>Hylobates albibarbis</i>	Extant
AMNH 103441	Hylobatidae	<i>Hylobates albibarbis</i>	Extant
AMNH 103665	Hylobatidae	<i>Hylobates albibarbis</i>	Extant
AMNH 106053	Hylobatidae	<i>Hylobates albibarbis</i>	Extant
AMNH 103243	Hylobatidae	<i>Hylobates klossii</i>	Extant
MCZ 41546	Hylobatidae	<i>Hylobates lar</i>	Extant
AMNH 54662	Hylobatidae	<i>Hylobates lar entelloides</i>	Extant
AMNH 101695	Hylobatidae	<i>Hylobates lar entelloides</i>	Extant
USNM 083262	Hylobatidae	<i>Hylobates lar entelloides</i>	Extant
USNM 111970	Hylobatidae	<i>Hylobates lar entelloides</i>	Extant
USNM 111989	Hylobatidae	<i>Hylobates lar entelloides</i>	Extant
USNM 124232	Hylobatidae	<i>Hylobates lar entelloides</i>	Extant
USNM 296922	Hylobatidae	<i>Hylobates lar entelloides</i>	Extant
USNM 296923	Hylobatidae	<i>Hylobates lar entelloides</i>	Extant
AMNH 102093	Hylobatidae	<i>Hylobates moloch</i>	Extant
AMNH 41342	Hylobatidae	<i>Hylobates moloch</i>	Extant
ZMB 7808	Hylobatidae	<i>Hylobates muelleri</i>	Extant
AMNH 103403	Hylobatidae	<i>Hylobates muelleri</i>	Extant
AMNH 103723	Hylobatidae	<i>Hylobates muelleri</i>	Extant
AMNH 106782	Hylobatidae	<i>Hylobates muelleri</i>	Extant
AMNH 106327	Hylobatidae	<i>Hylobates muelleri</i>	Extant
USNM 198268	Hylobatidae	<i>Hylobates muelleri funereus</i>	Extant
USNM 241019	Hylobatidae	<i>Hylobates pileatus</i>	Extant
USNM 296920	Hylobatidae	<i>Hylobates pileatus</i>	Extant
ZMB 7814	Hylobatidae	<i>Hylobates</i> sp. indet.	Extant
ZMB 7860	Hylobatidae	<i>Hylobates</i> sp. indet.	Extant
ZMB 7825	Hylobatidae	<i>Hylobates</i> sp. indet.	Extant

ZMB 7819	Hylobatidae	<i>Hylobates</i> sp. indet.	Extant
MCZ 38115	Hylobatidae	<i>Nomascus concolor</i>	Extant
MCZ 38116	Hylobatidae	<i>Nomascus concolor</i>	Extant
KIZ 000170	Hylobatidae	<i>Nomascus concolor</i>	Extant
KIZ 000391	Hylobatidae	<i>Nomascus concolor</i>	Extant
KIZ 003192	Hylobatidae	<i>Nomascus concolor</i>	Extant
KIZ 009643	Hylobatidae	<i>Nomascus concolor</i>	Extant
KIZ 0106167	Hylobatidae	<i>Nomascus concolor</i>	Extant
KIZ 012168	Hylobatidae	<i>Nomascus concolor</i>	Extant
USNM 464992	Hylobatidae	<i>Nomascus concolor</i>	Extant
AMNH 87252	Hylobatidae	<i>Nomascus gabriellae</i>	Extant
SYS 1	Hylobatidae	<i>Nomascus hainanus</i>	Extant
IOZ 14517	Hylobatidae	<i>Nomascus leucogenys</i>	Extant
IOZ 18071	Hylobatidae	<i>Nomascus leucogenys</i>	Extant
KIZ 000175	Hylobatidae	<i>Nomascus leucogenys</i>	Extant
USNM 240490	Hylobatidae	<i>Nomascus leucogenys</i>	Extant
AMNH 102195	Hylobatidae	<i>Symphalangus syndactylus</i>	Extant
AMNH 102196	Hylobatidae	<i>Symphalangus syndactylus</i>	Extant
AMNH 102197	Hylobatidae	<i>Symphalangus syndactylus</i>	Extant
AMNH 102720	Hylobatidae	<i>Symphalangus syndactylus</i>	Extant
AMNH 102724	Hylobatidae	<i>Symphalangus syndactylus</i>	Extant
AMNH 102725	Hylobatidae	<i>Symphalangus syndactylus</i>	Extant
USNM 395514	Hylobatidae	<i>Symphalangus syndactylus</i>	Extant
USNM 519573	Hylobatidae	<i>Symphalangus syndactylus</i>	Extant
MCZ 27831	Hylobatidae	<i>Symphalangus syndactylus</i>	Extant
MCZ 17684	Hominidae	<i>Gorilla gorilla</i>	Extant
MCZ 38326	Hominidae	<i>Gorilla gorilla</i>	Extant
MCZ 46325	Hominidae	<i>Gorilla gorilla</i>	Extant
ZMB 30941	Hominidae	<i>Gorilla gorilla</i>	Extant
ZMB 31626	Hominidae	<i>Gorilla gorilla</i>	Extant
AMNH 115609	Hominidae	<i>Gorilla gorilla</i>	Extant
AMNH 167325	Hominidae	<i>Gorilla gorilla</i>	Extant
AMNH 167326	Hominidae	<i>Gorilla gorilla</i>	Extant
AMNH 167327	Hominidae	<i>Gorilla gorilla</i>	Extant
AMNH 167328	Hominidae	<i>Gorilla gorilla</i>	Extant
AMNH 167332	Hominidae	<i>Gorilla gorilla</i>	Extant
AMNH 167337	Hominidae	<i>Gorilla gorilla</i>	Extant
AMNH 167338	Hominidae	<i>Gorilla gorilla</i>	Extant
AMNH 167339	Hominidae	<i>Gorilla gorilla</i>	Extant
AMNH 167672	Hominidae	<i>Gorilla gorilla</i>	Extant
AMNH 170363	Hominidae	<i>Gorilla gorilla</i>	Extant
AMNH 200503	Hominidae	<i>Gorilla gorilla</i>	Extant
AMNH 200506	Hominidae	<i>Gorilla gorilla</i>	Extant
AMNH 201472	Hominidae	<i>Gorilla gorilla</i>	Extant
AMNH 214104	Hominidae	<i>Gorilla gorilla</i>	Extant
AMNH 214107	Hominidae	<i>Gorilla gorilla</i>	Extant

AMNH 214111	Hominidae	<i>Gorilla gorilla</i>	Extant
AMNH 214113	Hominidae	<i>Gorilla gorilla</i>	Extant
AMNH 235603	Hominidae	<i>Gorilla gorilla</i>	Extant
AMNH 54089	Hominidae	<i>Gorilla gorilla</i>	Extant
AMNH 54090	Hominidae	<i>Gorilla gorilla</i>	Extant
AMNH 90194	Hominidae	<i>Gorilla gorilla</i>	Extant
ZMB 31277	Hominidae	<i>Gorilla gorilla</i>	Extant
ZMB 31435	Hominidae	<i>Gorilla gorilla</i>	Extant
ZMB 83546	Hominidae	<i>Gorilla gorilla</i>	Extant
ZMB 83561	Hominidae	<i>Gorilla gorilla</i>	Extant
AMNH 51376	Hominidae	<i>Pan troglodytes</i>	Extant
MCZ 9493	Hominidae	<i>Pan troglodytes</i>	Extant
MCZ 6244	Hominidae	<i>Pan troglodytes</i>	Extant
AMNH 119227	Hominidae	<i>Pan troglodytes</i>	Extant
AMNH 167342	Hominidae	<i>Pan troglodytes</i>	Extant
AMNH 167346	Hominidae	<i>Pan troglodytes</i>	Extant
AMNH 183130	Hominidae	<i>Pan troglodytes</i>	Extant
AMNH 51204	Hominidae	<i>Pan troglodytes</i>	Extant
AMNH 51376	Hominidae	<i>Pan troglodytes</i>	Extant
AMNH 51377	Hominidae	<i>Pan troglodytes</i>	Extant
AMNH 51394	Hominidae	<i>Pan troglodytes</i>	Extant
AMNH 81854	Hominidae	<i>Pan troglodytes</i>	Extant
AMNH 89353	Hominidae	<i>Pan troglodytes</i>	Extant
AMNH 89406	Hominidae	<i>Pan troglodytes</i>	Extant
AMNH 90293	Hominidae	<i>Pan troglodytes</i>	Extant
MCZ 37518	Hominidae	<i>Pongo pygmaeus</i>	Extant
MCZ 37519	Hominidae	<i>Pongo pygmaeus</i>	Extant
AMNH 19548	Hominidae	<i>Pongo pygmaeus</i>	Extant
AMNH 28253	Hominidae	<i>Pongo pygmaeus</i>	Extant
USNM 142169	Hominidae	<i>Pongo pygmaeus</i>	Extant
USNM 142191	Hominidae	<i>Pongo pygmaeus</i>	Extant
USNM 142195	Hominidae	<i>Pongo pygmaeus</i>	Extant
ZMB 6954	Hominidae	<i>Pongo pygmaeus</i>	Extant
ZMB 6957	Hominidae	<i>Pongo pygmaeus</i>	Extant
ZMB 83509	Hominidae	<i>Pongo pygmaeus</i>	Extant

Table S2. List of catarrhine M₃ specimens included in this study.

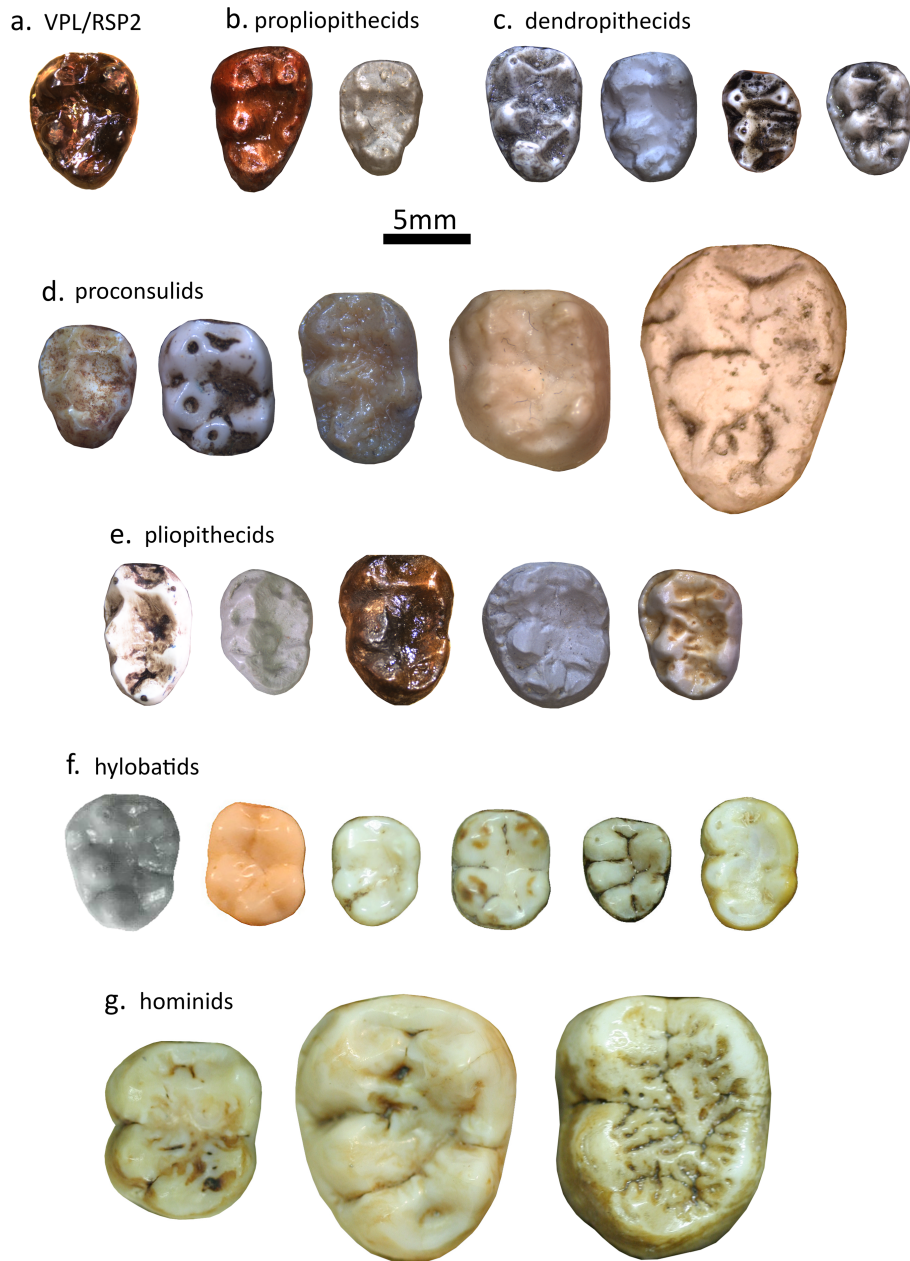


Figure S2. *Kapi ramnagarensis* gen. et sp. nov. in occlusal view compared to a sample of extinct and extant catarrhines. All specimens are M_3S and are visualized with the buccal side to the left (right molars mirror-imaged and identified with *). **a**, VPL/RSP2 from Ramnagar, India; **b**, propliopithecids (left to right): *Aegyptopithecus zeuxis* (DPC 2806), *Propliopithecus chirobates* (DPC 1069); **c**, dendropithecids (left to right): *Dendropithecus* sp. indet. (KNM-ZP 01669b*), *Limnopithecus evansi* (KNM-SO 444*), *Micropithecus leakeyorum* (KNM-MB 9767*), *Simiolus enjiessi* (KNM-WK 16960)*; **d**, proconsulids (left to right): *Kalepithecus songhorensis* (KNM-SO 378*), *Ekembo heseloni* (KNM-RU 7290), *Rangwapithecus gordoni* (KNM-SO 463*), *Otavipithecus namibiensis* (BERI*), *Proconsul major* (KNM-SO 396); **e**, pliopithecids (left to right): *Egarapithecus narcisoi* (IPS 2943*), *Epipliopithecus vindobenensis* (Naturhistorisches Museum, Basel, Individual I), *Laccopithecus robustus* (PA 880), *Platodontopithecus jianghuaiensis* (PA 870), *Pliopithecus antiquus* (MNHN Chantrei Deperet, La Grive)*; **f**, hylobatids (left to right): *Yuanmoupithecus* (YML 112-1x; image from Pan, 2006), *Bunopithecus sericus* (AMNH 18534), *Nomascus leucogenys* (NMNH 240490), *Hoolock hoolock* (AMNH 83413), *Hylobates moloch* (AMNH 103442), *Symphalangus syndactylus* (USNM 519573*); **g**, hominids (from left to right): *Pan troglodytes* (AMNH 167342), *Gorilla gorilla* (AMNH 167338), *Pongo pygmaeus* (NMNH 142195).

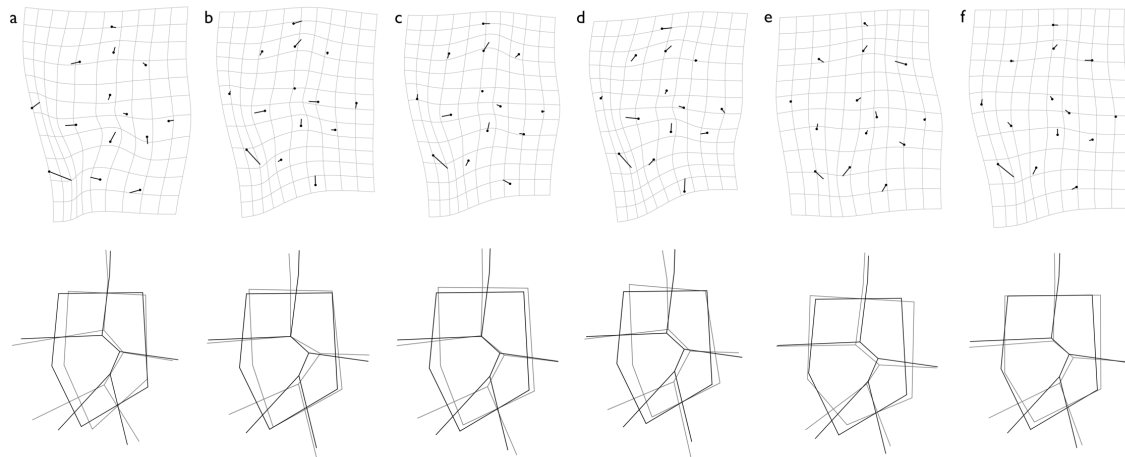


Figure S3. Deformation grids (top row) and wireframes (bottom row) based on 14 homologous landmarks (14L) comparing VPL/RSP2 with: **a**, propliopithecids; **b**, proconsulids; **c**, dendropithecids; **d**, pliopithecids; **e**, hylobatids; and **f**, hominids. Deformation grids show shape deformations from the M₃ mean shape (reference configuration) of each of the five major taxonomic groups analyzed to the M₃ shape of VPL/RSP2 (target configuration), with vectors indicating the direction of change from the reference to the target shape coordinate locations. Wireframes compare the M₃ configuration of VPL/RSP2 (in black) with mean shapes of extant and extinct catarrhine taxa (in gray). Procrustes distances for a (0.16), b (0.15), c (0.14), d (0.16), e (0.11), and f (0.12); *p*-values non-significant.

Specimen	PC1	PC2	PC3	PC4	PC5	PC6
<i>Kapi</i> VPL/RSP2	-0.0181	-0.0283	0.0371	0.0152	-0.0081	0.0215
<i>Dendropithecus</i> KNM-RU 2015	0.0740	0.0431	0.0091	-0.0103	0.0270	0.0144
<i>Dendropithecus</i> KNM-ZP 01669	0.0269	0.0487	0.0055	0.0718	-0.0685	0.0017
<i>Dendropithecus</i> KNM-RU 16650	0.0147	0.0549	0.0182	0.0507	-0.0090	-0.0169
<i>Limnopithecus</i> KNM-SO 444	0.0421	-0.0477	-0.0152	0.0579	0.0017	0.0323
<i>Limnopithecus</i> KNM-ZP 01675	0.0539	0.0161	0.0282	0.0174	-0.0090	0.0080
<i>Micropithecus</i> KNM MB 9767	0.0809	-0.0048	0.0025	-0.0632	-0.0108	0.0174
<i>Simiolus</i> KNM-WK 16960	0.1208	-0.0614	-0.0093	0.0333	0.0386	-0.0018
<i>Bunopithecus</i> AMNH 18534	-0.1091	0.0064	0.0421	0.0673	0.0196	0.0154
<i>Hoolock</i> AMNH 112671	-0.1677	0.0668	-0.0160	0.0526	-0.0106	0.0465
<i>Hoolock</i> AMNH 112674	-0.0338	-0.0207	0.0057	-0.0088	0.0127	0.0040
<i>Hoolock</i> AMNH 112680	-0.0717	0.0212	0.0348	0.0075	0.0086	0.0202
<i>Hoolock</i> AMNH 112683	-0.0679	0.0170	0.0486	0.0233	0.0065	0.0424
<i>Hoolock</i> AMNH 112688	-0.0211	0.0384	0.0062	0.0025	0.0311	-0.0041
<i>Hoolock</i> AMNH 112697	-0.1222	-0.0724	0.0476	0.0254	-0.0107	-0.0422
<i>Hoolock</i> AMNH 112698	-0.0609	-0.0202	0.0517	0.0367	-0.0301	0.0016
<i>Hoolock</i> AMNH 112702	-0.0907	0.0349	0.0039	-0.0131	0.0090	0.0125
<i>Hoolock</i> AMNH 112703	-0.0487	0.0038	0.0178	-0.0026	0.0509	0.0438
<i>Hoolock</i> AMNH 112719	-0.0547	0.0030	-0.0022	-0.0064	-0.0121	0.0129
<i>Hoolock</i> AMNH 112720	-0.0224	-0.0011	0.0473	-0.0106	0.0224	0.0289
<i>Hoolock</i> AMNH 112960	0.0375	-0.0188	0.0513	-0.0816	0.0124	0.0001
<i>Hoolock</i> AMNH 83413	-0.0702	0.0473	0.0449	-0.0151	-0.0217	-0.0113
<i>Hoolock</i> AMNH 83415	-0.0436	-0.0712	0.0038	0.0136	0.0000	-0.0326
<i>Hoolock</i> AMNH 83417	-0.0681	0.0145	0.0318	0.0393	-0.0265	0.0365
<i>Hoolock</i> KIZ 014035	-0.0642	-0.0413	0.0433	0.0480	0.0186	-0.0013
<i>Hoolock</i> USNM 257988	-0.0539	-0.1388	-0.0122	0.0471	-0.0136	-0.0040
<i>Hylobates</i> AMNH 101695	-0.0597	-0.0661	0.0313	0.0181	-0.0194	-0.0080
<i>Hylobates</i> AMNH 102093	-0.0442	-0.0768	0.0062	-0.0087	-0.0239	0.0254
<i>Hylobates</i> AMNH 102161	-0.0125	0.0258	0.0092	-0.0479	0.0103	-0.0012
<i>Hylobates</i> AMNH 102200	-0.0076	-0.0442	-0.0576	-0.0316	0.0323	0.0297
<i>Hylobates</i> AMNH 102773	-0.0473	-0.0398	-0.0731	-0.0472	0.0567	-0.0160
<i>Hylobates</i> AMNH 102774	-0.0539	0.0333	-0.0274	-0.0681	0.0280	0.0258
<i>Hylobates</i> AMNH 103243	-0.0927	-0.0214	0.0244	0.0392	-0.0117	0.0045
<i>Hylobates</i> AMNH 103403	-0.0468	-0.0006	0.0007	-0.0618	0.0337	0.0056
<i>Hylobates</i> AMNH 103441	-0.0792	0.0427	-0.0333	-0.0499	0.0394	-0.0221
<i>Hylobates</i> AMNH 103442	0.0132	0.0176	-0.0111	-0.0673	0.0141	-0.0224
<i>Hylobates</i> AMNH 103665	0.0359	-0.0038	0.0226	-0.0697	-0.0326	0.0101
<i>Hylobates</i> AMNH 103723	-0.0914	0.0001	0.0094	0.0134	-0.0518	-0.0088
<i>Hylobates</i> AMNH 106053	-0.0815	-0.0255	0.0141	-0.0199	-0.0232	-0.0140
<i>Hylobates</i> AMNH 106327	-0.0245	-0.0611	0.0468	-0.0263	-0.0127	-0.0266
<i>Hylobates</i> AMNH 106571	-0.1073	0.0007	-0.1018	0.0173	-0.0006	0.0331
<i>Hylobates</i> AMNH 106572	-0.0196	-0.0044	-0.0027	-0.0464	-0.0089	-0.0215
<i>Hylobates</i> AMNH 106578	-0.0151	0.0124	-0.0227	-0.0508	0.0040	-0.0085
<i>Hylobates</i> AMNH 106678	-0.0039	-0.0298	-0.0352	-0.0381	0.0060	0.0026
<i>Hylobates</i> AMNH 106679	-0.0394	0.0458	-0.0747	0.0045	-0.0074	-0.0001

<i>Hylobates</i> AMNH 106782	-0.0617	-0.0794	0.0441	-0.0486	-0.0049	-0.0360
<i>Hylobates</i> AMNH 41342	-0.0829	-0.0526	0.0194	-0.0187	-0.0472	0.0197
<i>Hylobates</i> AMNH 54662	-0.0067	-0.0020	0.0098	-0.0575	-0.0014	-0.0005
<i>Hylobates</i> MCZ 41546	-0.0123	0.0247	0.0068	-0.0569	0.0223	0.0373
<i>Hylobates</i> USNM 083262	-0.0590	-0.0612	0.0361	0.0065	-0.0435	0.0203
<i>Hylobates</i> USNM 111970	-0.0204	-0.0191	0.0266	0.0057	-0.0356	0.0033
<i>Hylobates</i> USNM 111989	-0.0456	-0.0002	-0.0826	0.0206	0.0140	0.0001
<i>Hylobates</i> USNM 124232	-0.0515	-0.0369	0.0456	0.0070	0.0304	0.0088
<i>Hylobates</i> USNM 198268	-0.0405	-0.0177	-0.0297	-0.0114	0.0092	-0.0235
<i>Hylobates</i> USNM 241019	-0.0059	-0.0452	0.0197	-0.0892	0.0278	-0.0143
<i>Hylobates</i> USNM 296920	-0.0362	-0.0289	-0.0415	0.0391	0.0144	-0.0173
<i>Hylobates</i> USNM 296922	-0.0498	0.0413	-0.0077	-0.0364	0.0004	0.0089
<i>Hylobates</i> USNM 296923	-0.0884	-0.0339	0.0078	0.0388	0.0140	0.0168
<i>Hylobates</i> ZMB 7814	-0.0777	0.0157	0.0176	-0.0155	-0.0351	0.0042
<i>Hylobates</i> ZMB 7819	0.0221	-0.0734	-0.0308	-0.0266	-0.0234	-0.0029
<i>Hylobates</i> ZMB 7825	-0.0474	0.0214	-0.0084	0.0004	-0.0014	0.0169
<i>Hylobates</i> ZMB 7860	-0.0752	-0.0049	-0.0339	0.0108	-0.0176	-0.0307
<i>Hylobates</i> ZMB 7808	-0.1112	0.0340	0.0352	-0.0115	0.0179	0.0405
<i>Nomascus</i> KIZ000175	-0.0951	-0.0616	-0.0379	0.0636	-0.0316	-0.0198
<i>Nomascus</i> AMNH 87252	-0.0515	0.0316	0.0312	-0.0230	0.0273	0.0395
<i>Nomascus</i> IOZ 14517	-0.0805	-0.0128	0.0167	0.0380	0.0678	-0.0080
<i>Nomascus</i> IOZ 18071	-0.0508	0.0117	0.0014	0.0284	0.0313	-0.0427
<i>Nomascus</i> KIZ 000170	-0.0609	-0.0442	-0.0068	0.0189	0.0196	0.0025
<i>Nomascus</i> KIZ 000391	0.0061	-0.0193	-0.0306	0.0097	0.0151	0.0002
<i>Nomascus</i> KIZ 003192	-0.0613	-0.0073	0.0062	-0.0133	0.0427	0.0153
<i>Nomascus</i> KIZ 009643	-0.0628	-0.0078	0.0021	-0.0014	0.0401	-0.0231
<i>Nomascus</i> KIZ 0106167	-0.0653	-0.0654	-0.0206	-0.0100	0.0113	-0.0271
<i>Nomascus</i> KIZ 012168	0.0067	-0.0373	-0.0471	-0.0088	0.0343	-0.0198
<i>Nomascus</i> MCZ 38115	-0.0369	0.0331	0.0504	-0.0072	-0.0226	0.0147
<i>Nomascus</i> MCZ 38116	-0.0556	-0.0147	-0.0183	0.0172	-0.0007	0.0115
<i>Nomascus</i> SYS1	-0.1167	0.1150	-0.0007	0.0547	0.0656	0.0281
<i>Nomascus</i> USNM 240490	-0.0227	0.0417	-0.0327	-0.0337	-0.0257	0.0091
<i>Nomascus</i> USNM 464992	-0.0679	-0.0538	-0.0554	0.0391	-0.0090	-0.0020
<i>Symphalangus</i> AMNH 102195	-0.0076	0.0733	-0.1379	-0.0236	-0.0429	0.0396
<i>Symphalangus</i> AMNH 102196	-0.0178	0.0042	-0.0440	0.0252	-0.0010	0.0487
<i>Symphalangus</i> AMNH 102197	0.0168	0.0235	-0.0840	0.0564	-0.0210	0.0233
<i>Symphalangus</i> AMNH 102720	0.0543	0.0253	-0.0146	-0.0270	0.0009	0.0300
<i>Symphalangus</i> AMNH 102724	0.0341	0.0304	-0.0204	-0.0207	-0.0343	0.0122
<i>Symphalangus</i> AMNH 102725	0.0173	0.0318	-0.0370	0.0384	-0.0521	0.0360
<i>Symphalangus</i> MCZ 27831	-0.0349	0.0165	-0.0357	0.0100	-0.0290	0.0197
<i>Symphalangus</i> USNM 395514	-0.0239	-0.0540	-0.0140	0.0391	-0.0233	0.0116
<i>Symphalangus</i> USNM 519573	0.0502	0.0261	-0.0448	-0.0127	-0.0544	0.0433
<i>Yuanmoupithecus</i> YML 112-1x	0.0340	-0.0039	-0.0220	0.0318	0.0185	0.0744
<i>Anapithecus</i> RUD 98	0.0645	-0.0861	0.0708	0.1061	-0.0202	-0.0015
<i>Egarapithecus</i> IPS 2943	0.0890	-0.0600	0.0203	-0.0116	-0.0760	0.0739
<i>Epipliopithecus</i> NM (Basel) Ind I	0.1105	-0.0010	0.0120	0.0229	0.0284	0.0057
<i>Epipliopithecus</i> NM (Basel) Ind III	0.1771	-0.0160	0.0321	-0.0040	0.0031	0.0148
<i>Laccopithecus</i> PA 880	0.0984	-0.0513	0.0335	0.0667	0.0527	0.0007

<i>Platodontopithecus</i> PA 870	0.0399	0.0793	0.0603	0.0400	0.0148	0.0134
<i>Pliopithecus</i> Goriach (H30)	0.0745	0.0068	0.0515	0.0777	0.0241	0.0404
<i>Pliopithecus</i> La Grive	0.0583	-0.0625	0.0611	-0.0189	0.0504	0.0340
<i>Pliopithecus</i> MNHN Sansan (H2)	0.1549	-0.0398	0.0885	-0.0302	0.0256	-0.0057
<i>Ekembo</i> KNM-RU 1674	0.0562	0.0264	0.0565	0.0322	-0.0095	0.0046
<i>Ekembo</i> KNM-RU 1947	0.0958	0.0027	-0.0089	-0.0235	0.0406	0.0283
<i>Ekembo</i> KNM-RU 7290	0.1512	-0.0249	0.0071	-0.0237	0.0426	0.0357
<i>Kalepithecus</i> KNM-SO 378	0.0645	0.0309	0.0500	0.0396	0.0211	0.0231
<i>Otavipithecus</i> BER I	0.0475	-0.0527	0.0408	-0.0030	0.0066	0.0188
<i>Proconsul</i> KNM-SO 396	0.0813	-0.0366	0.0275	0.0366	-0.0171	-0.0125
<i>Rangwapithecus</i> KNM-SO 463	0.1469	-0.0174	0.0501	0.0109	-0.0243	0.0646
<i>Aegyptopithecus</i> DPC 1027	0.0801	0.0161	0.0183	0.0615	0.0678	-0.0425
<i>Aegyptopithecus</i> DPC 2806	0.0700	0.0047	-0.0137	0.0749	-0.0171	-0.0315
<i>Aegyptopithecus</i> YPM 21032	0.0749	0.0550	0.0843	0.0685	-0.0396	-0.0396
<i>Aegyptopithecus</i> DPC 1028	0.0514	0.0724	0.0036	0.0769	0.0261	-0.0182
<i>Propliopithecus</i> DPC 1069	0.0118	0.0440	-0.0430	0.0684	-0.0008	-0.0604
<i>Propliopithecus</i> DPC 5392	0.0171	0.0765	0.0257	0.1068	0.0243	-0.0756
<i>Gorilla</i> MCZ 17684	0.0546	0.0050	-0.0175	-0.0038	-0.0450	-0.0448
<i>Gorilla</i> MCZ 38326	0.0500	-0.0127	-0.0634	-0.0249	-0.0461	-0.0065
<i>Gorilla</i> MCZ 46325	0.0246	-0.0336	-0.0673	-0.0273	-0.0033	0.0307
<i>Gorilla</i> ZMB 30941	0.0314	0.0395	-0.0422	0.0187	0.0136	-0.0489
<i>Gorilla</i> ZMB 31626	0.0657	-0.0037	0.0108	-0.0542	-0.0184	-0.0389
<i>Gorilla</i> AMNH 115609	0.0350	0.0407	-0.0280	0.0122	-0.0236	-0.0133
<i>Gorilla</i> AMNH 167325	0.0688	0.0086	-0.0672	0.0364	-0.0036	0.0574
<i>Gorilla</i> AMNH 167326	0.0421	-0.0679	-0.0658	0.0113	0.0083	-0.0143
<i>Gorilla</i> AMNH 167327	0.0150	0.0419	-0.0343	0.0205	0.0258	-0.0282
<i>Gorilla</i> AMNH 167328	0.0177	-0.0105	-0.0202	0.0128	-0.0394	-0.0395
<i>Gorilla</i> AMNH 167332	0.0296	0.0246	-0.0357	-0.0161	-0.0383	0.0044
<i>Gorilla</i> AMNH 167337	0.0209	-0.0018	-0.0797	-0.0020	-0.0114	0.0218
<i>Gorilla</i> AMNH 167338	0.0285	-0.0107	-0.0461	0.0066	0.0124	-0.0089
<i>Gorilla</i> AMNH 167339	0.0422	-0.0900	-0.0442	0.0296	0.0222	0.0196
<i>Gorilla</i> AMNH 167672	0.0503	0.0031	-0.0380	0.0104	0.0163	-0.0103
<i>Gorilla</i> AMNH 170363	-0.0395	0.0131	-0.0324	-0.0463	0.0601	0.0026
<i>Gorilla</i> AMNH 200503	0.0517	0.0100	-0.0159	0.0104	-0.0375	0.0216
<i>Gorilla</i> AMNH 200506	0.0524	0.0407	-0.0402	-0.0128	-0.0272	-0.0256
<i>Gorilla</i> AMNH 201472	0.0072	-0.0079	-0.0636	0.0301	0.0098	-0.0603
<i>Gorilla</i> AMNH 214104	0.0567	0.0144	-0.0374	-0.0163	-0.0554	-0.0692
<i>Gorilla</i> AMNH 214107	0.0405	0.0524	-0.0038	0.0124	-0.0008	0.0006
<i>Gorilla</i> AMNH 214111	0.0674	0.0007	0.0440	-0.0307	-0.0047	0.0048
<i>Gorilla</i> AMNH 214113	0.0182	-0.0184	-0.0452	-0.0446	-0.0022	-0.0376
<i>Gorilla</i> AMNH 235603	0.0948	0.0277	-0.0267	0.0160	0.0366	-0.0193
<i>Gorilla</i> AMNH 54089	0.0498	0.0123	0.0268	-0.0229	-0.0004	-0.0306
<i>Gorilla</i> AMNH 54090	0.0203	-0.0486	-0.0133	-0.0182	-0.0022	-0.0348
<i>Gorilla</i> AMNH 90194	0.0567	-0.0703	-0.0106	-0.0659	0.0128	0.0018
<i>Gorilla</i> ZMB 31277	0.0897	-0.0179	-0.0655	-0.0217	-0.0097	-0.0267
<i>Gorilla</i> ZMB 31435	0.0542	-0.0149	-0.0205	-0.0230	-0.0383	-0.0696
<i>Gorilla</i> ZMB 83546	-0.0376	0.0161	-0.0294	0.0070	0.0136	-0.0370
<i>Gorilla</i> ZMB 83561	0.0155	0.0203	-0.0264	0.0133	0.0205	-0.0097

<i>Pan</i> AMNH 51376	0.0163	0.0736	0.0308	-0.0558	-0.0177	-0.0126
<i>Pan</i> MCZ 9493	-0.0027	0.0038	0.0442	-0.0408	-0.0268	-0.0099
<i>Pan</i> MCZ 6244	0.0216	0.0275	0.0171	0.0575	0.0109	-0.0139
<i>Pan</i> AMNH 119227	-0.0157	0.0470	0.0269	-0.0336	-0.0094	0.0243
<i>Pan</i> AMNH 167342	-0.0411	-0.0011	0.0093	-0.0426	-0.0173	-0.0109
<i>Pan</i> AMNH 167346	-0.0721	0.0491	0.0802	-0.0521	0.0404	-0.0233
<i>Pan</i> AMNH 183130	0.0184	0.0002	0.0251	-0.0267	0.0559	-0.0324
<i>Pan</i> AMNH 51204	-0.0549	0.0210	0.0241	-0.0120	-0.0771	0.0182
<i>Pan</i> AMNH 51376	0.0056	0.0796	0.0286	-0.0478	-0.0134	-0.0113
<i>Pan</i> AMNH 51377	-0.0071	0.0092	0.0385	-0.0209	-0.0179	-0.0564
<i>Pan</i> AMNH 51394	-0.0921	0.0176	0.0449	-0.0287	0.0104	-0.0248
<i>Pan</i> AMNH 81854	-0.0296	0.0344	0.0513	-0.0505	-0.0404	-0.0121
<i>Pan</i> AMNH 89353	-0.0048	-0.0027	0.0540	-0.0722	-0.0158	-0.0187
<i>Pan</i> AMNH 89406	-0.0065	0.0255	0.0503	-0.0475	-0.0201	-0.0327
<i>Pan</i> AMNH 90293	-0.0595	0.0192	0.0640	-0.0033	-0.0094	0.0112
<i>Pongo</i> MCZ 37518	0.0191	-0.0115	-0.0375	-0.0118	0.0534	0.0370
<i>Pongo</i> MCZ 37519	0.0227	0.0469	-0.0155	-0.0154	0.0650	0.0023
<i>Pongo</i> AMNH 19548	0.0281	-0.0379	0.0302	0.0139	0.0124	-0.0179
<i>Pongo</i> AMNH 28253	0.0413	0.0518	-0.0101	0.0078	0.0006	-0.0407
<i>Pongo</i> USNM 142169	0.0301	0.0404	0.0039	0.0211	0.0031	-0.0139
<i>Pongo</i> USNM 142191	0.1151	0.0578	0.0030	-0.0421	0.0106	0.0245
<i>Pongo</i> USNM 142195	0.0152	0.0197	0.0485	0.0205	-0.0556	0.0056
<i>Pongo</i> ZMB 6954	0.0809	-0.0072	-0.0234	-0.0227	-0.0042	0.0228
<i>Pongo</i> ZMB 6957	0.0348	0.0526	0.0211	-0.0034	-0.0475	0.0125

Table S3. Results of M₃ PCA including PC scores by specimen for the first 6 PCs.

Specimen number	Family	Genus and species	Fossil/Extant
H-GSP 8114-609	Incertae sedis	<i>"Dionysopithecus" sp. indet.</i>	Fossil
DPC 1112	Propliopithecidae	<i>Aegyptopithecus zeuxis</i>	Fossil
YPM 21032	Propliopithecidae	<i>Aegyptopithecus zeuxis</i>	Fossil
DPC 1028	Propliopithecidae	<i>Aegyptopithecus zeuxis</i>	Fossil
DPC 1069	Propliopithecidae	<i>Propliopithecus chirobates</i>	Fossil
DPC 1106	Propliopithecidae	<i>Propliopithecus chirobates</i>	Fossil
DPC 1029	Propliopithecidae	<i>Propliopithecus sp. indet.</i>	Fossil
KNM-RU 2015	Dendropithecidae	<i>Dendropithecus macinnesi</i>	Fossil
KNM-RU 1850	Dendropithecidae	<i>Dendropithecus macinnesi</i>	Fossil
KNM-RU 1727	Dendropithecidae	<i>Dendropithecus macinnesi</i>	Fossil
KNM-RU 900	Dendropithecidae	<i>Dendropithecus macinnesi</i>	Fossil
KNM-ZP 01669	Dendropithecidae	<i>Dendropithecus sp. indet.</i>	Fossil
KNM-KO 8	Dendropithecidae	<i>Limnopithecus legetet</i>	Fossil
KNM-ZP 01675	Dendropithecidae	<i>Limnopithecus sp. indet.</i>	Fossil
KNM-LG 920	Dendropithecidae	<i>Micropithecus clarki</i>	Fossil
KNM-ZP 10670	Dendropithecidae	<i>Micropithecus sp. indet.</i>	Fossil
KNM-WK 16960	Dendropithecidae	<i>Simiolus enjiessi</i>	Fossil
KNM-RU 7290	Proconsulidae	<i>Ekembo heseloni</i>	Fossil
KNM-RU 1678	Proconsulidae	<i>Ekembo heseloni</i>	Fossil
KNM-RU 2036	Proconsulidae	<i>Ekembo heseloni</i>	Fossil
KNM-MB 20573	Proconsulidae	<i>Equatorius</i>	Fossil
KNM-NC 9740	Proconsulidae	<i>Equatorius africanus</i>	Fossil
KNM-TH 28860	Proconsulidae	<i>Equatorius africanus</i>	Fossil
KNM-SO 378	Proconsulidae	<i>Kalepithicus</i>	Fossil
BER I	Proconsulidae	<i>Otavipithecus</i>	Fossil
KNM-RU 1706	Proconsulidae	<i>Proconsul africanus</i>	Fossil
KNM-SO 396	Proconsulidae	<i>Proconsul major</i>	Fossil
KNM-SO 464	Proconsulidae	<i>Rangwapithecus gordonii</i>	Fossil
TF 2451	Pliopithecidae	<i>"Dionysopithecus" orientalis</i>	Fossil
PA 1054	Pliopithecidae	<i>Dionysopithecus shuangouensis</i>	Fossil
PA 1243	Pliopithecidae	<i>Dionysopithecus shuangouensis</i>	Fossil
PA 1251	Pliopithecidae	<i>Dionysopithecus shuangouensis</i>	Fossil
PA 1224	Pliopithecidae	<i>Platodontopithecus jianghuaiensis</i>	Fossil
PA 1225	Pliopithecidae	<i>Platodontopithecus jianghuaiensis</i>	Fossil
PA 1226	Pliopithecidae	<i>Platodontopithecus jianghuaiensis</i>	Fossil
Sa 999 (MNHN)	Pliopithecidae	<i>Plesiopithecus auscitanensis</i>	Fossil
IPS 41719	Pliopithecidae	<i>Pliopithecus canmatensis</i>	Fossil
Goriach (H24)	Pliopithecidae	<i>Pliopithecus platydon</i>	Fossil
Goriach (H30), Joanneum 3675	Pliopithecidae	<i>Pliopithecus platydon</i>	Fossil
Goriach (H32), Joanneum 2100	Pliopithecidae	<i>Pliopithecus platydon</i>	Fossil
AMNH 19400	Hylobatidae	<i>Hoolock sp. indet.</i>	Extant
AMNH 112689	Hylobatidae	<i>Hoolock hoolock</i>	Extant
AMNH 112691	Hylobatidae	<i>Hoolock hoolock</i>	Extant
AMNH 112699	Hylobatidae	<i>Hoolock hoolock</i>	Extant
AMNH 112700	Hylobatidae	<i>Hoolock hoolock</i>	Extant

AMNH 112703	Hylobatidae	<i>Hoolock hoolock</i>	Extant
AMNH 83414	Hylobatidae	<i>Hoolock hoolock</i>	Extant
AMNH 83424	Hylobatidae	<i>Hoolock hoolock</i>	Extant
AMNH 112669	Hylobatidae	<i>Hoolock leuconedys</i>	Extant
AMNH 112671	Hylobatidae	<i>Hoolock leuconedys</i>	Extant
AMNH 112677	Hylobatidae	<i>Hoolock leuconedys</i>	Extant
AMNH 112965	Hylobatidae	<i>Hoolock leuconedys</i>	Extant
KIZ 011796	Hylobatidae	<i>Hoolock leuconedys</i>	Extant
KIZ 011345	Hylobatidae	<i>Hoolock sp. indet.</i>	Extant
USNM 111990	Hylobatidae	<i>Hoolock sp. indet.</i>	Extant
KIZ 011338	Hylobatidae	<i>Hoolock tianxing</i>	Extant
MCZ 26474	Hylobatidae	<i>Hoolock tianxing</i>	Extant
AMNH 102161	Hylobatidae	<i>Hylobates agilis</i>	Extant
AMNH 102162	Hylobatidae	<i>Hylobates agilis</i>	Extant
AMNH 102200	Hylobatidae	<i>Hylobates agilis</i>	Extant
AMNH 102473	Hylobatidae	<i>Hylobates agilis</i>	Extant
AMNH 102474	Hylobatidae	<i>Hylobates agilis</i>	Extant
AMNH 102775	Hylobatidae	<i>Hylobates agilis</i>	Extant
AMNH 102776	Hylobatidae	<i>Hylobates agilis</i>	Extant
AMNH 102777	Hylobatidae	<i>Hylobates agilis</i>	Extant
AMNH 106679	Hylobatidae	<i>Hylobates agilis</i>	Extant
USNM 113177	Hylobatidae	<i>Hylobates agilis</i>	Extant
AMNH 103442	Hylobatidae	<i>Hylobates albibarbis</i>	Extant
AMNH 103443	Hylobatidae	<i>Hylobates albibarbis</i>	Extant
AMNH 103454	Hylobatidae	<i>Hylobates albibarbis</i>	Extant
AMNH 103353	Hylobatidae	<i>Hylobates klossii</i>	Extant
AMNH 43063	Hylobatidae	<i>Hylobates lar</i>	Extant
AMNH 43064	Hylobatidae	<i>Hylobates lar</i>	Extant
AMNH 54662	Hylobatidae	<i>Hylobates lar</i>	Extant
AMNH 54966	Hylobatidae	<i>Hylobates lar</i>	Extant
KIZ 003147	Hylobatidae	<i>Hylobates lar</i>	Extant
USNM 83262	Hylobatidae	<i>Hylobates lar</i>	Extant
USNM 296922	Hylobatidae	<i>Hylobates lar</i>	Extant
AMNH 102026	Hylobatidae	<i>Hylobates moloch</i>	Extant
AMNH 106788	Hylobatidae	<i>Hylobates moloch</i>	Extant
AMNH 130172	Hylobatidae	<i>Hylobates moloch</i>	Extant
AMNH 200853	Hylobatidae	<i>Hylobates moloch</i>	Extant
ZMB 7835	Hylobatidae	<i>Hylobates muelleri</i>	Extant
ZMB 7804	Hylobatidae	<i>Hylobates muelleri</i>	Extant
USNM 198268	Hylobatidae	<i>Hylobates muelleri</i>	Extant
USNM 198271	Hylobatidae	<i>Hylobates muelleri</i>	Extant
USNM 198272	Hylobatidae	<i>Hylobates muelleri</i>	Extant
USNM 198843	Hylobatidae	<i>Hylobates muelleri</i>	Extant
UNSM 201556	Hylobatidae	<i>Hylobates pileatus</i>	Extant
USNM 253405	Hylobatidae	<i>Hylobates pileatus</i>	Extant
ZMB 7819	Hylobatidae	<i>Hylobates sp. indet.</i>	Extant
AMNH 100048	Hylobatidae	<i>Hylobates sp. indet.</i>	Extant
MCZ 38114	Hylobatidae	<i>Nomascus concolor</i>	Extant

MCZ 38115	Hylobatidae	<i>Nomascus concolor</i>	Extant
IOZ 17927	Hylobatidae	<i>Nomascus concolor</i>	Extant
IOZ 17929	Hylobatidae	<i>Nomascus concolor</i>	Extant
KIZ 000170	Hylobatidae	<i>Nomascus concolor</i>	Extant
KIZ 000391	Hylobatidae	<i>Nomascus concolor</i>	Extant
KIZ 010122	Hylobatidae	<i>Nomascus concolor</i>	Extant
KIZ 010122-LS980628	Hylobatidae	<i>Nomascus concolor</i>	Extant
KIZ 024165	Hylobatidae	<i>Nomascus concolor</i>	Extant
USNM 320787	Hylobatidae	<i>Nomascus concolor</i>	Extant
USNM 464992	Hylobatidae	<i>Nomascus concolor</i>	Extant
USNM 257996	Hylobatidae	<i>Nomascus gabriellae</i>	Extant
IOZ 14524	Hylobatidae	<i>Nomascus leucogenys</i>	Extant
IOZ 14525	Hylobatidae	<i>Nomascus leucogenys</i>	Extant
KIZ 000173	Hylobatidae	<i>Nomascus leucogenys</i>	Extant
KIZ 000175	Hylobatidae	<i>Nomascus leucogenys</i>	Extant
USNM 296921	Hylobatidae	<i>Nomascus leucogenys</i>	Extant
ZMB 38586	Hylobatidae	<i>Symphalangus syndactylus</i>	Extant
AMNH 102189	Hylobatidae	<i>Symphalangus syndactylus</i>	Extant
AMNH 102193	Hylobatidae	<i>Symphalangus syndactylus</i>	Extant
AMNH 102722	Hylobatidae	<i>Symphalangus syndactylus</i>	Extant
MCZ 36031	Hylobatidae	<i>Symphalangus syndactylus</i>	Extant
AMNH 115609	Hominidae	<i>Gorilla gorilla</i>	Extant
AMNH 167326	Hominidae	<i>Gorilla gorilla</i>	Extant
AMNH 167328	Hominidae	<i>Gorilla gorilla</i>	Extant
AMNH 167333	Hominidae	<i>Gorilla gorilla</i>	Extant
AMNH 167334	Hominidae	<i>Gorilla gorilla</i>	Extant
AMNH 167337	Hominidae	<i>Gorilla gorilla</i>	Extant
AMNH 167338	Hominidae	<i>Gorilla gorilla</i>	Extant
AMNH 167339	Hominidae	<i>Gorilla gorilla</i>	Extant
AMNH 200506	Hominidae	<i>Gorilla gorilla</i>	Extant
AMNH 235603	Hominidae	<i>Gorilla gorilla</i>	Extant
AMNH 54089	Hominidae	<i>Gorilla gorilla</i>	Extant
AMNH 54090	Hominidae	<i>Gorilla gorilla</i>	Extant
AMNH 54091	Hominidae	<i>Gorilla gorilla</i>	Extant
AMNH 90194	Hominidae	<i>Gorilla gorilla</i>	Extant
ZMB 31435	Hominidae	<i>Gorilla gorilla</i>	Extant
ZMB 83546	Hominidae	<i>Gorilla gorilla</i>	Extant
AMNH 119227	Hominidae	<i>Pan troglodytes</i>	Extant
AMNH 167342	Hominidae	<i>Pan troglodytes</i>	Extant
AMNH 167345	Hominidae	<i>Pan troglodytes</i>	Extant
AMNH 183130	Hominidae	<i>Pan troglodytes</i>	Extant
AMNH 201239	Hominidae	<i>Pan troglodytes</i>	Extant
AMNH 35199	Hominidae	<i>Pan troglodytes</i>	Extant
AMNH 3550	Hominidae	<i>Pan troglodytes</i>	Extant
AMNH 5094	Hominidae	<i>Pan troglodytes</i>	Extant
AMNH 51204	Hominidae	<i>Pan troglodytes</i>	Extant
AMNH 51208	Hominidae	<i>Pan troglodytes</i>	Extant
AMNH 51211	Hominidae	<i>Pan troglodytes</i>	Extant

AMNH 51377	Hominidae	<i>Pan troglodytes</i>	Extant
AMNH 51382	Hominidae	<i>Pan troglodytes</i>	Extant
AMNH 51386	Hominidae	<i>Pan troglodytes</i>	Extant
AMNH 51392	Hominidae	<i>Pan troglodytes</i>	Extant
AMNH 89352	Hominidae	<i>Pan troglodytes</i>	Extant
AMNH 89353	Hominidae	<i>Pan troglodytes</i>	Extant
AMNH 89406	Hominidae	<i>Pan troglodytes</i>	Extant
AMNH 89407	Hominidae	<i>Pan troglodytes</i>	Extant
AMNH 90191	Hominidae	<i>Pan troglodytes</i>	Extant
AMNH 90293	Hominidae	<i>Pan troglodytes</i>	Extant
AMNH 19548	Hominidae	<i>Pongo pygmaeus</i>	Extant
AMNH 18010	Hominidae	<i>Pongo pygmaeus</i>	Extant
AMNH 19180	Hominidae	<i>Pongo pygmaeus</i>	Extant
AMNH 202511	Hominidae	<i>Pongo pygmaeus</i>	Extant
AMNH 28253	Hominidae	<i>Pongo pygmaeus</i>	Extant
AMNH 35549	Hominidae	<i>Pongo pygmaeus</i>	Extant
AMNH 80008	Hominidae	<i>Pongo pygmaeus</i>	Extant
USNM 142170	Hominidae	<i>Pongo pygmaeus</i>	Extant
USNM 142191	Hominidae	<i>Pongo pygmaeus</i>	Extant
USNM 142195	Hominidae	<i>Pongo pygmaeus</i>	Extant
USNM 142196	Hominidae	<i>Pongo pygmaeus</i>	Extant
USNM 142200	Hominidae	<i>Pongo pygmaeus</i>	Extant
USNM 142169	Hominidae	<i>Pongo pygmaeus</i>	Extant
USNM 145319	Hominidae	<i>Pongo pygmaeus</i>	Extant
ZMB 67173	Hominidae	<i>Pongo pygmaeus</i>	Extant
ZMB 6954	Hominidae	<i>Pongo pygmaeus</i>	Extant
ZMB 6957	Hominidae	<i>Pongo pygmaeus</i>	Extant

Table S4. List of catarrhine M₁ specimens included in this study.

M₃ Analysis

PC	Eigenvalue	% variance	SUM Variance
1	0.0038	25.08%	25.08%
2	0.0017	10.84%	35.91%
3	0.0016	10.32%	46.23%
4	0.0015	9.60%	55.82%
5	0.0009	5.76%	61.59%
6	0.0008	5.08%	66.66%
7	0.0006	3.96%	70.62%
8	0.0006	3.64%	74.26%
9	0.0005	3.22%	77.47%
10	0.0004	2.87%	80.34%
11	0.0004	2.59%	82.92%
12	0.0003	2.27%	85.19%
13	0.0003	2.19%	87.39%
14	0.0003	2.11%	89.50%
15	0.0003	1.71%	91.21%
16	0.0002	1.45%	92.66%
17	0.0002	1.40%	94.05%
18	0.0002	1.25%	95.30%
19	0.0002	1.15%	96.45%
20	0.0002	0.99%	97.44%
21	0.0001	0.84%	98.28%
22	0.0001	0.80%	99.08%
23	0.0001	0.62%	99.70%
24	0.0000	0.31%	100.00%

M₁ Analysis

PC	Eigenvalue	% variance	SUM Variance
1	0.0021	21.19%	21.19%
2	0.0014	14.38%	35.56%
3	0.0008	8.62%	44.18%
4	0.0007	7.58%	51.75%
5	0.0006	6.06%	57.81%
6	0.0005	5.17%	62.98%

7	0.0004	4.35%	67.33%
8	0.0004	3.96%	71.28%
9	0.0004	3.81%	75.09%
10	0.0003	3.37%	78.46%
11	0.0003	3.07%	81.54%
12	0.0003	2.55%	84.08%
13	0.0002	2.38%	86.47%
14	0.0002	1.91%	88.37%
15	0.0002	1.85%	90.22%
16	0.0002	1.60%	91.82%
17	0.0001	1.40%	93.22%
18	0.0001	1.33%	94.55%
19	0.0001	1.27%	95.82%
20	0.0001	1.12%	96.93%
21	0.0001	1.01%	97.94%
22	0.0001	0.94%	98.88%
23	0.0001	0.65%	99.52%
24	0.0000	0.48%	100.00%

Table S5. Principal Components loadings and Eigenvalues for 14L 2D GM analyses of M₃ and M₁ specimens.

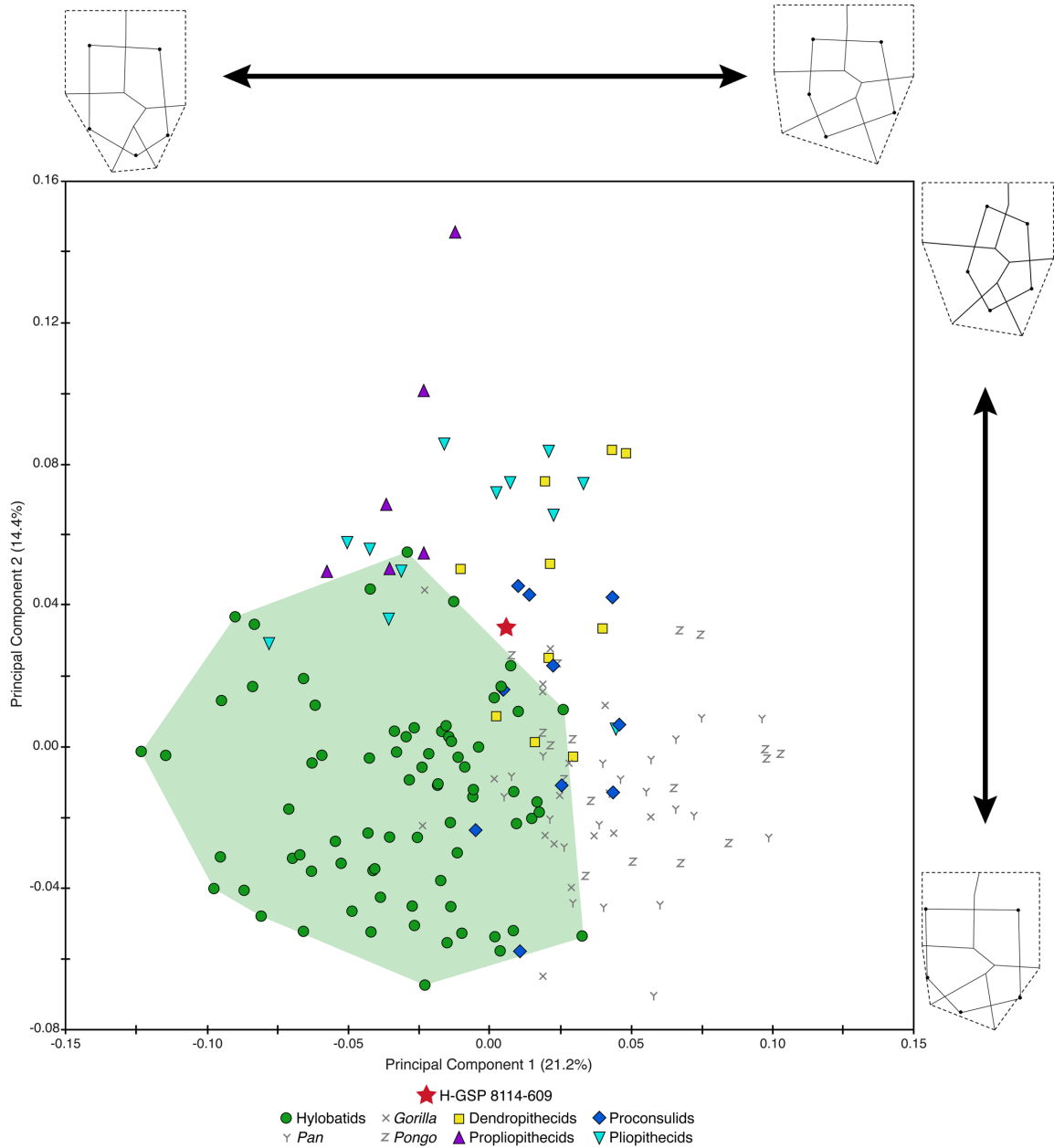


Figure S4. PCA resulting from 2D morphometric analysis of overall M₁ crown shape characterized by 14 homologous landmarks (see wireframes; cusps=black circles). H-GSP 8114-609 *Dionysopithecus* sp. plots within the area of overlap between multiple stem and crown catarrhine/hominoid families, but outside the distribution of hylobatid specimens (=green polygon).

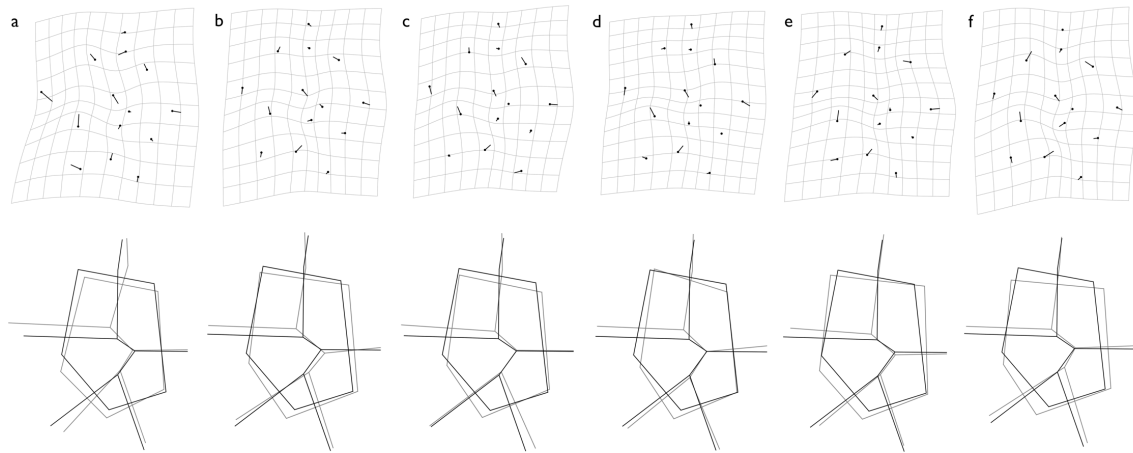


Figure S5. Deformation grids (top row) and wireframes (bottom row) based on 14 homologous landmarks (14L) comparing H-GSP 8114-609 (*Dionysopithecus* sp. indet.) with: **a**, propliopithecids; **b**, proconsulids; **c**, dendropithecids; **d**, pliopithecids; **e**, hylobatids; and **f**, hominids. Deformation grids show shape deformations from the M₁ mean shape (reference configuration) of each of the five major taxonomic groups analyzed to the M₁ shape of H-GSP 8114-609 (target configuration), with vectors indicating the direction of change from the reference to the target shape coordinate locations. Wireframes compare the M₁ configuration of H-GSP 8114-609 (in black) with mean shapes of extant and extinct catarrhine taxa (in gray). Procrustes distances for a (0.15), b (0.10), c (0.10), d (0.10), and e (0.12); and f (0.12); *p*-values non-significant.

Specimen	PC1	PC2	PC3	PC4	PC5	PC6
<i>Dendropithecus</i> KNM-RU 1727	0.0214	0.0518	0.0063	0.0386	0.0073	0.0070
<i>Dendropithecus</i> KNM-RU 1850	0.0482	0.0831	0.0276	0.0364	0.0180	0.0147
<i>Dendropithecus</i> KNM-RU 2015	-0.0103	0.0503	0.0376	-0.0043	-0.0183	-0.0103
<i>Dendropithecus</i> KNM-RU 900	0.0196	0.0751	-0.0231	0.0002	0.0189	-0.0147
<i>Dendropithecus</i> KNM-ZP 01669	0.0295	-0.0028	-0.0093	-0.0380	0.0398	-0.0165
<i>Limnopithecus</i> KNM-KO 8	0.0400	0.0335	-0.0131	0.0261	0.0027	0.0161
<i>Limnopithecus</i> KNM-ZP 01675	0.0433	0.0840	0.0267	0.0326	0.0337	-0.0005
<i>Micropithecus</i> KNM-LG 920	0.0023	0.0087	0.0203	-0.0008	0.0059	-0.0222
<i>Micropithecus</i> KNM-ZP 01670	0.0160	0.0013	0.0195	0.0232	0.0000	-0.0449
<i>Simiolus</i> KNM-WK 16960	0.0209	0.0252	0.0495	0.0355	-0.0036	-0.0301
" <i>Dionysopithecus</i> " H-GSP 8114-609	0.0059	0.0340	0.0226	-0.0303	-0.0134	0.0074
<i>Hoolock</i> AMNH 112669	-0.0137	-0.0452	0.0538	-0.0105	-0.0172	0.0049
<i>Hoolock</i> AMNH 112671	-0.0425	-0.0032	-0.0624	-0.0358	-0.0163	0.0215
<i>Hoolock</i> AMNH 112677	-0.0295	0.0029	-0.0304	-0.0304	-0.0009	0.0167
<i>Hoolock</i> AMNH 112689	0.0260	0.0106	-0.0505	-0.0176	0.0298	0.0261
<i>Hoolock</i> AMNH 112691	0.0016	0.0139	-0.0303	-0.0304	-0.0235	0.0388
<i>Hoolock</i> AMNH 112699	-0.0144	0.0029	-0.0066	-0.0189	0.0308	0.0274
<i>Hoolock</i> AMNH 112700	0.0149	-0.0202	-0.0370	-0.0358	0.0298	0.0359
<i>Hoolock</i> AMNH 112703	-0.0154	0.0060	-0.0398	-0.0012	-0.0168	-0.0028
<i>Hoolock</i> AMNH 112965	-0.0173	-0.0378	0.0148	-0.0232	-0.0312	0.0149
<i>Hoolock</i> AMNH 19400	-0.0127	0.0411	-0.0136	-0.0146	-0.0071	-0.0014
<i>Hoolock</i> AMNH 83414	0.0041	0.0171	-0.0551	-0.0333	0.0478	0.0030
<i>Hoolock</i> AMNH 83424	-0.0088	-0.0057	-0.0134	-0.0235	0.0282	0.0029
<i>Hoolock</i> KIZ 011338	-0.0617	0.0118	-0.0174	-0.0126	0.0082	0.0311
<i>Hoolock</i> KIZ 011345	-0.0710	-0.0176	-0.0069	-0.0204	-0.0034	0.0365
<i>Hoolock</i> KIZ 011796	-0.0658	0.0193	-0.0390	0.0343	-0.0349	0.0057
<i>Hoolock</i> MCZ 26474	-0.0291	0.0551	-0.0085	-0.0141	0.0417	0.0090
<i>Hoolock</i> USNM 111990	-0.0659	-0.0522	-0.0077	-0.0051	-0.0095	-0.0061
<i>Hylobates</i> AMNH 100048	-0.0671	-0.0305	0.0992	-0.0059	0.0292	-0.0098
<i>Hylobates</i> AMNH 102026	-0.0135	0.0016	0.0066	0.0063	-0.0221	0.0111
<i>Hylobates</i> AMNH 102161	0.0176	-0.0185	-0.0176	-0.0005	0.0195	0.0089
<i>Hylobates</i> AMNH 102162	-0.0114	-0.0300	-0.0316	0.0016	-0.0024	0.0414
<i>Hylobates</i> AMNH 102200	-0.0697	-0.0315	0.0092	0.0251	0.0259	0.0148
<i>Hylobates</i> AMNH 102473	-0.0150	-0.0554	-0.0519	0.0072	-0.0372	-0.0042
<i>Hylobates</i> AMNH 102474	-0.0975	-0.0401	0.0172	-0.0162	-0.0177	-0.0111
<i>Hylobates</i> AMNH 102775	-0.1146	-0.0024	-0.0480	-0.0379	-0.0649	0.0256
<i>Hylobates</i> AMNH 102776	-0.0139	-0.0214	0.0031	-0.0197	0.0069	0.0139
<i>Hylobates</i> AMNH 102777	-0.0229	-0.0674	0.0530	-0.0119	-0.0066	0.0089
<i>Hylobates</i> AMNH 103353	-0.0239	-0.0057	-0.0035	-0.0168	0.0138	0.0021
<i>Hylobates</i> AMNH 103442	-0.0413	-0.0350	-0.0416	-0.0098	-0.0441	0.0125
<i>Hylobates</i> AMNH 103443	-0.1232	-0.0013	0.0038	-0.0028	-0.0047	0.0243
<i>Hylobates</i> AMNH 103454	0.0085	-0.0127	-0.0364	0.0316	0.0186	-0.0012
<i>Hylobates</i> AMNH 106679	0.0084	-0.0520	-0.0077	-0.0545	0.0149	-0.0073
<i>Hylobates</i> AMNH 106788	0.0168	-0.0156	-0.0069	-0.0033	0.0101	-0.0330
<i>Hylobates</i> AMNH 130172	-0.0284	-0.0093	-0.0112	-0.0168	-0.0043	0.0087
<i>Hylobates</i> AMNH 200853	-0.0060	-0.0141	-0.0096	-0.0105	-0.0166	-0.0156
<i>Hylobates</i> AMNH 43063	-0.0948	0.0131	-0.0599	0.0010	0.0336	-0.0136

<i>Hylobates</i> AMNH 43064	-0.0900	0.0368	-0.0851	0.0003	0.0219	-0.0378
<i>Hylobates</i> AMNH 54662	-0.0256	-0.0256	-0.0136	-0.0243	0.0329	-0.0293
<i>Hylobates</i> AMNH 54966	-0.0182	-0.0105	-0.0135	-0.0077	-0.0031	0.0151
<i>Hylobates</i> KIZ 003147	-0.0832	0.0347	-0.0355	-0.0625	0.0115	-0.0158
<i>Hylobates</i> USNM 083262	-0.0267	0.0054	-0.0232	0.0351	-0.0375	-0.0143
<i>Hylobates</i> USNM 113177	-0.0266	-0.0505	-0.0441	0.0058	-0.0280	0.0044
<i>Hylobates</i> USNM 198268	0.0037	-0.0577	0.0497	-0.0005	-0.0320	-0.0215
<i>Hylobates</i> USNM 198271	-0.0098	-0.0527	0.0462	0.0009	0.0274	-0.0094
<i>Hylobates</i> USNM 198272	-0.0630	-0.0352	0.0028	0.0169	-0.0327	0.0420
<i>Hylobates</i> USNM 198843	-0.0112	-0.0029	-0.0296	-0.0039	0.0193	-0.0112
<i>Hylobates</i> USNM 201556	-0.0329	-0.0015	0.0532	0.0174	0.0285	-0.0089
<i>Hylobates</i> USNM 253405	-0.0838	0.0171	0.0266	0.0265	0.0074	0.0172
<i>Hylobates</i> USNM 296922	-0.0487	-0.0465	-0.0260	0.0444	0.0215	-0.0577
<i>Hylobates</i> ZMB 7804	0.0327	-0.0535	0.0100	0.0112	0.0314	-0.0138
<i>Hylobates</i> ZMB 7819	-0.0420	-0.0524	-0.0007	0.0175	-0.0203	0.0168
<i>Hylobates</i> ZMB 7835	-0.0868	-0.0406	-0.0203	-0.0067	0.0213	-0.0458
<i>Nomascus</i> IOZ 14524	-0.0169	0.0044	0.0247	-0.0376	-0.0068	0.0255
<i>Nomascus</i> IOZ 14525	-0.0058	-0.0121	0.0438	-0.0194	0.0478	0.0029
<i>Nomascus</i> IOZ 17927	-0.0430	-0.0244	0.0661	0.0070	-0.0398	0.0062
<i>Nomascus</i> IOZ 17929	-0.0525	-0.0329	0.0538	0.0369	-0.0181	-0.0183
<i>Nomascus</i> KIZ 000170	-0.0274	-0.0450	0.0428	0.0107	-0.0264	0.0222
<i>Nomascus</i> KIZ 000173	-0.0215	-0.0019	0.0137	-0.0036	-0.0071	0.0423
<i>Nomascus</i> KIZ 000175	-0.0184	-0.0108	0.0240	-0.0314	-0.0093	0.0187
<i>Nomascus</i> KIZ 000391	-0.0546	-0.0267	-0.0043	0.0174	-0.0071	0.0036
<i>Nomascus</i> KIZ 010122	-0.0422	0.0447	-0.0149	0.0180	0.0406	0.0276
<i>Nomascus</i> KIZ 010122-LS980628	-0.0593	-0.0024	-0.0131	0.0213	0.0342	-0.0058
<i>Nomascus</i> KIZ 024165	-0.0406	-0.0345	0.0027	-0.0158	-0.0072	0.0143
<i>Nomascus</i> MCZ 38114	0.0075	0.0230	0.0214	-0.0557	0.0310	0.0004
<i>Nomascus</i> MCZ 38115	0.0095	-0.0217	0.0111	-0.0335	-0.0106	-0.0110
<i>Nomascus</i> USNM 257996	-0.0354	-0.0255	-0.0188	-0.0054	0.0255	-0.0063
<i>Nomascus</i> USNM 296921	-0.0808	-0.0479	0.0364	0.0167	-0.0059	0.0063
<i>Nomascus</i> USNM 320787	-0.0952	-0.0311	-0.0012	0.0269	-0.0134	-0.0056
<i>Nomascus</i> USNM 464992	-0.0628	-0.0046	0.0257	-0.0028	0.0240	0.0210
<i>Symphalangus</i> AMNH 102189	0.0101	0.0100	0.0115	-0.0113	0.0426	-0.0016
<i>Symphalangus</i> AMNH 102193	0.0019	-0.0537	0.0263	0.0315	0.0431	0.0246
<i>Symphalangus</i> AMNH 102722	-0.0337	0.0044	-0.0082	-0.0277	0.0376	-0.0222
<i>Symphalangus</i> MCZ 36031	-0.0039	0.0000	0.0037	0.0072	0.0809	-0.0113
<i>Symphalangus</i> ZMB 38586	-0.0386	-0.0425	0.0505	0.0217	0.0080	0.0070
<i>Dionysopithecus</i> PA 1054	-0.0504	0.0579	0.0491	-0.0395	-0.0128	0.0039
<i>Dionysopithecus</i> PA 1243	0.0024	0.0720	0.0192	-0.0190	0.0383	0.0051
<i>Dionysopithecus</i> PA 1251	0.0073	0.0749	-0.0020	-0.0619	0.0104	-0.0184
<i>Dionysopithecus</i> TF 2451	0.0447	0.0051	0.0107	0.0133	0.0210	-0.0300
<i>Platodontopithecus</i> PA 1224	0.0332	0.0746	0.0037	-0.0360	-0.0030	0.0105
<i>Platodontopithecus</i> PA 1225	0.0226	0.0657	0.0431	-0.0441	-0.0025	0.0382
<i>Platodontopithecus</i> PA 1226	0.0209	0.0837	0.0164	-0.0553	-0.0151	0.0092
<i>Plesiopithecus</i> MNHN Sa 999	-0.0780	0.0293	0.0236	-0.0069	0.0070	-0.0200
<i>Pliopithecus</i> Goriach (H24)	-0.0160	0.0858	0.0090	0.0102	-0.0414	0.0179
<i>Pliopithecus</i> Goriach (H30)	-0.0312	0.0499	0.0242	-0.0159	-0.0094	-0.0322
<i>Pliopithecus</i> Goriach (H32)	-0.0357	0.0363	0.0168	-0.0304	-0.0473	-0.0906

<i>Pliopithecus</i> IPS 41719	-0.0424	0.0560	0.0516	0.0031	-0.0081	-0.0045
<i>Ekembo</i> KNM-RU 1678	0.0225	0.0230	0.0268	-0.0231	-0.0111	0.0108
<i>Ekembo</i> KNM-RU 7290	0.0047	0.0162	0.0008	-0.0291	-0.0208	0.0003
<i>Equatorius</i> KNM-MB 20573	0.0107	-0.0578	-0.0277	0.0067	-0.0316	-0.0039
<i>Equatorius</i> KNM-NC 9740	-0.0050	-0.0235	0.0470	0.0023	-0.0210	-0.0387
<i>Equatorius</i> KNM-TH 28860	0.0101	0.0455	0.0340	0.0005	-0.0162	-0.0186
<i>Kalepithecus</i> KNM-SO 378	0.0435	0.0423	0.0326	-0.0209	0.0047	-0.0094
<i>Otavipithecus</i> BER I	0.0459	0.0063	0.0314	-0.0244	-0.0056	0.0112
<i>Proconsul</i> KNM-RU 1706	0.0437	-0.0129	0.0296	0.0162	-0.0239	-0.0135
<i>Proconsul</i> KNM-RU 2036	0.0255	-0.0109	0.0134	0.0022	0.0255	-0.0028
<i>Proconsul</i> KNM-SO 396	0.0140	0.0430	-0.0171	0.0008	-0.0175	0.0004
<i>Rangwapithecus</i> KNM-SO 464	0.0049	0.0162	0.0219	0.0164	0.0379	0.0108
<i>Aegyptopithecus</i> YPM 21032	-0.0233	0.0547	-0.0461	0.0571	-0.0004	-0.0313
<i>Aegyptopithecus</i> DPC 1028	-0.0233	0.1007	-0.0001	0.0554	-0.0408	-0.0051
<i>Aegyptopithecus</i> DPC 1112	-0.0366	0.0685	0.0063	0.0285	-0.0273	0.0013
<i>Propliopithecus</i> DPC 1029	-0.0122	0.1455	-0.0531	0.0573	-0.0403	-0.0175
<i>Propliopithecus</i> DPC 1069	-0.0575	0.0495	-0.0318	0.0239	-0.0279	-0.0102
<i>Propliopithecus</i> DPC 1106	-0.0354	0.0503	-0.0095	-0.0166	-0.0117	-0.0288
<i>Gorilla</i> AMNH 115609	0.0409	0.0117	0.0272	0.0392	0.0110	-0.0184
<i>Gorilla</i> AMNH 167326	0.0228	-0.0275	-0.0097	0.0372	0.0279	0.0197
<i>Gorilla</i> AMNH 167328	0.0289	-0.0398	-0.0052	0.0395	0.0374	0.0164
<i>Gorilla</i> AMNH 167333	0.0570	-0.0198	-0.0048	-0.0145	0.0068	0.0123
<i>Gorilla</i> AMNH 167334	0.0189	-0.0649	-0.0081	0.0254	-0.0116	0.0005
<i>Gorilla</i> AMNH 167337	-0.0237	-0.0223	-0.0137	0.0154	0.0023	0.0072
<i>Gorilla</i> AMNH 167338	0.0370	-0.0252	-0.0093	0.0271	0.0099	0.0288
<i>Gorilla</i> AMNH 167339	0.0196	-0.0250	0.0164	0.0242	0.0088	0.0385
<i>Gorilla</i> AMNH 200506	0.0188	0.0156	-0.0131	-0.0069	0.0143	0.0383
<i>Gorilla</i> AMNH 235603	0.0189	0.0177	-0.0149	-0.0007	0.0086	0.0205
<i>Gorilla</i> AMNH 54089	0.0016	-0.0090	-0.0039	0.0130	-0.0092	-0.0135
<i>Gorilla</i> AMNH 54090	0.0281	-0.0046	0.0110	0.0296	-0.0112	0.0069
<i>Gorilla</i> AMNH 54091	0.0215	0.0278	0.0146	0.0424	-0.0086	0.0179
<i>Gorilla</i> AMNH 90194	0.0439	-0.0244	-0.0119	0.0299	0.0356	0.0122
<i>Gorilla</i> ZMB 31435	0.0248	-0.0137	-0.0178	0.0614	0.0257	0.0246
<i>Gorilla</i> ZMB 83546	-0.0230	0.0444	0.0026	0.0875	0.0454	0.0300
<i>Pan</i> AMNH 119227	0.0213	-0.0204	-0.0162	0.0337	-0.0069	-0.0133
<i>Pan</i> AMNH 167342	0.0051	-0.0141	-0.0278	0.0029	-0.0033	0.0012
<i>Pan</i> AMNH 167345	0.0077	-0.0083	-0.0056	-0.0284	0.0134	-0.0075
<i>Pan</i> AMNH 183130	0.0963	0.0080	-0.0057	0.0084	-0.0406	0.0384
<i>Pan</i> AMNH 201239	0.0987	-0.0256	-0.0470	0.0141	-0.0035	-0.0133
<i>Pan</i> AMNH 35199	0.0554	-0.0126	0.0247	-0.0391	0.0058	0.0061
<i>Pan</i> AMNH 3550	0.0603	-0.0446	-0.0304	0.0558	0.0042	0.0068
<i>Pan</i> AMNH 5094	0.0580	-0.0704	-0.0391	0.0229	-0.0244	-0.0388
<i>Pan</i> AMNH 51204	0.0189	-0.0025	-0.0304	0.0022	-0.0303	0.0285
<i>Pan</i> AMNH 51208	0.0264	-0.0283	-0.0182	-0.0270	-0.0212	-0.0116
<i>Pan</i> AMNH 51211	0.0403	-0.0453	-0.0065	-0.0722	0.0017	-0.0057
<i>Pan</i> AMNH 51377	0.0659	0.0022	0.0084	0.0220	-0.0333	-0.0010
<i>Pan</i> AMNH 51382	0.0750	0.0082	0.0009	0.0236	0.0035	0.0193
<i>Pan</i> AMNH 51386	0.0295	-0.0441	-0.0006	0.0178	-0.0184	-0.0246
<i>Pan</i> AMNH 51392	0.0723	-0.0194	-0.0223	-0.0156	-0.0109	-0.0009

<i>Pan</i> AMNH 89352	0.0388	-0.0220	0.0140	-0.0265	0.0109	-0.1035
<i>Pan</i> AMNH 89353	0.0571	-0.0036	-0.0189	-0.0053	-0.0119	-0.0341
<i>Pan</i> AMNH 89406	0.0400	-0.0046	-0.0471	-0.0125	0.0398	-0.0178
<i>Pan</i> AMNH 89407	0.0658	-0.0176	-0.0282	-0.0342	-0.0419	0.0103
<i>Pan</i> AMNH 90191	0.0424	-0.0131	-0.0357	0.0183	-0.0099	-0.0272
<i>Pan</i> AMNH 90293	0.0463	-0.0091	-0.0344	0.0185	-0.0024	-0.0028
<i>Pongo</i> AMNH 19548	0.0358	-0.0153	0.0199	0.0124	-0.0249	-0.0185
<i>Pongo</i> AMNH 18010	0.0293	0.0022	-0.0324	-0.0023	0.0237	-0.0054
<i>Pongo</i> AMNH 19180	0.0676	-0.0329	-0.0091	-0.0156	-0.0254	-0.0264
<i>Pongo</i> AMNH 202511	0.0652	-0.0117	-0.0008	-0.0207	0.0021	-0.0239
<i>Pongo</i> AMNH 28253	0.0262	-0.0091	0.0265	0.0398	-0.0308	-0.0018
<i>Pongo</i> AMNH 35549	0.0846	-0.0272	-0.0057	0.0142	-0.0027	0.0024
<i>Pongo</i> AMNH 80008	0.0339	-0.0365	-0.0071	-0.0325	-0.0067	-0.0027
<i>Pongo</i> USNM 142170	0.0215	0.0004	0.0235	0.0219	-0.0009	0.0015
<i>Pongo</i> USNM 142191	0.0746	0.0317	0.0027	0.0151	-0.0143	-0.0086
<i>Pongo</i> USNM 142195	0.0672	0.0330	0.0132	-0.0085	0.0012	0.0035
<i>Pongo</i> USNM 142196	0.0077	0.0259	0.0236	0.0003	-0.0123	-0.0192
<i>Pongo</i> USNM 142200	0.0975	-0.0007	0.0200	-0.0211	-0.0291	0.0348
<i>Pongo</i> USNM 142169	0.0506	-0.0325	0.0420	0.0078	0.0128	0.0185
<i>Pongo</i> USNM 145319	0.0980	-0.0033	0.0021	-0.0249	-0.0290	0.0190
<i>Pongo</i> ZMB 67173	0.0188	0.0040	-0.0046	0.0110	0.0024	-0.0123
<i>Pongo</i> ZMB 6954	0.1029	-0.0020	-0.0131	-0.0437	0.0041	0.0037
<i>Pongo</i> ZMB 6957	0.0240	0.0236	0.0064	0.0129	-0.0246	0.0241

Table S6. Results of M_1 PCA including PC scores by specimen for the first 6 PCs.